Age-related ultrastructural neurovascular changes in the female mouse cortex and hippocampus

Eduardo Frías-Anaya[1], Radka Gromnicova[1], Igor Kraev[1], Vadim Rogachevsky[2], David K. Male[1], Francesco Crea[1], Cheryl A. Hawkes[1,3], Ignacio A. Romero[1]

[1] School of Life, Health and Chemical Sciences, The Open University, Milton Keynes, UK

[2] Institute of Cell Biophysics RAS, Pushchino Federal Research Centre for Biological Research, Pushchino, Russia

[3] Department of Biomedical and Life Sciences, Lancaster University, Lancaster, UK

Eduardo Frías-Anaya: edufrias91@gmail.com

Radka Gromnicova: radka.gromnicova@open.ac.uk

Igor Kraev: igor.kraev@open.ac.uk

Vadim Rogachevsky: rog_v@mail.ru

David K. Male: david.male@open.ac.uk

Francesco Crea: francesco.crea@open.ac.uk

Cheryl A. Hawkes: c.hawkes@lancaster.ac.uk

Ignacio A. Romero (**corresponding author**): nacho.romero@open.ac.uk

Abbreviations: blood-brain barrier (BBB), brain endothelial cell (BEC), basement membrane (BM), phosphate buffer (PB), phosphate buffered saline (PBS), transmission electron microscopy (TEM).

Abstract

Blood-Brain Barrier (BBB) breakdown occurs in ageing and neurodegenerative diseases. Although age-associated alterations have previously been described, most studies focused in male brains; hence, little is known about BBB breakdown in females. This study measured ultrastructural features in the ageing female BBB using transmission electron microscopy (TEM) and 3D reconstruction of cortical and hippocampal capillaries from 6- and 24-month-old female C57BL/6J mice. Aged cortical capillaries showed more changes than hippocampal capillaries. Specifically, aged cortex showed thicker basement membrane (BM), higher number and volume of endothelial pseudopods, decreased endothelial mitochondrial number, larger pericyte mitochondria, higher pericyte – endothelial cell contact and increased tight junction tortuosity compared to young animals. Only increased BM thickness and pericyte mitochondrial volume were observed in aged hippocampus. Regional comparison revealed significant differences in endothelial pseudopods and tight junctions between cortex and hippocampus of 24-month-old mice. Therefore, the ageing female BBB shows region-specific ultrastructural alterations that may lead to oxidative stress and abnormal capillary blood flow and barrier stability, potentially contributing to cerebrovascular diseases, particularly in post-menopausal women.

Keywords: Aging, blood-brain barrier, capillary ultrastructure, female mouse, transmission electron microscopy, cerebrovasculature

1. Introduction

The blood-brain barrier (BBB) is a multicellular structure mainly composed of brain endothelial cells (BECs) that line cerebral microvessels, are tightly sealed together and, in association with pericytes and astrocyte end-feet, separate the brain parenchyma from the circulatory system (Abbott et al., 2006; Al Ahmad et al., 2011; Winkler et al., 2011; Wolburg and Lippoldt, 2002). This barrier limits paracellular transport via expression of continuous tight junctions between BECs, and modulates the entry of selected circulating ions, molecules, proteins and cells by specific transporters and receptors, thereby contributing to homeostasis of the central nervous system (Begley, 2004; Gee and Keller, 2005; Liebner et al., 2000b; Pardrige et al., 1990; Tsai et al., 2002). Dysfunction of the BBB is known to occur during normal ageing and in neurodegenerative disorders, including multiple sclerosis or Alzheimer´s disease (Popescu et al., 2009; Sweeney et al., 2018; Zlokovic, 2008).

Structural changes have been observed in almost every cellular and subcellular component of the aged BBB (Cullen et al., 2005; Montagne et al., 2015; Simpson et al., 2010). For example, early studies reported a significant decrease in the number of mitochondria in BECs in both the cortex and hippocampus of male rodents, primates and humans (Hicks et al., 1983). In addition, the luminal surface of BECs has been reported to become irregular in a senescence-accelerated mouse model, showing a higher presence of protrusions pinching off the cytoplasm towards the capillary lumen (Lee et al., 2000). The thickness of the basement membrane (BM) has also been reported to be significantly increased during ageing in microvessels of the brain and retina in mice and humans (Candiello et al., 2010; Ceafalan et al., 2019). Pericyte alterations appear to differ depending on the brain region and between species, with pericyte number being reported to decrease in human white matter but not grey matter (Farrell et al., 1987), whereas it has been observed to increase in male rat cortex (Peinado et al., 1998), or not to change at all in the brain of aged monkeys (Peters et al., 1991). In addition, pericyte area, coverage and contact with BECs have been described to decrease in aged male rodents and humans (Bell et al., 2010; Hughes et al., 2006; Stewart et al., 1987). In the ageing brain, astrocytes tend to show a swollen phenotype with thicker projections, accumulating in several regions including cortex and hippocampus (Amenta et al., 1998; Kanaan et al., 2010). Also, the process of

ageing has recently been described to promote neurovascular dysfunction by reducing astrocytic end-feet coverage over brain capillaries in male mice (Duncombe et al., 2017).

Despite women having a greater longevity (Regan and Partridge, 2013), higher prevalence of age-related neurodegenerative conditions such as Alzheimer's disease (Altmann et al., 2014; Paganini-hill and Henderson, 1994) and poorer prognosis after stroke (Reeves et al., 2008), very few studies have examined the effect of ageing on the female BBB. Higher capillary permeability, decreased expression of tight junction proteins occludin-1, zonula occludens-1 and claudin-5 and increased inflammation mediated by tumour necrosis factor-α have been reported in BECs of aged female rodents compared to younger female animals (Bake and Sohrabji, 2004; Elahy et al., 2015). Bake and colleagues also reported a more prominent decrease in claudin-5 expression in aged female rats compared to age-matched males (Bake et al., 2009). Sex steroid hormones have been described to target brain vessels (Krause et al., 2006; Wilson et al., 2008), and especially oestrogen and progesterone have been shown to play a protective role at the BBB by reducing oxidative stress and attenuating neuroinflammation, leukocyte migration, metalloproteinase activity and tight junction degradation (Corcoran et al., 2010; Gavin et al., 2009; He et al., 2004; Ishrat et al., 2010; Maggioli et al., 2016; Pascual et al., 2013; Razmara et al., 2008; Stirone et al., 2005). Accordingly, reduced production of oestrogen during reproductive senescence has been reported to promote loss of BBB integrity and altered transport within the female mouse brain (Kastin et al., 2001; Wilson et al., 2008). These findings suggest that the structure and integrity of the female BBB may be particularly vulnerable to age-related changes and associated cerebrovascular conditions.

As such, ultrastructural changes of the aged female BBB require additional investigation. The ultrastructure of the BBB is commonly assessed using transmission electron microscopy (TEM). Classical approaches involve collecting serial tissue sections which are then imaged at high resolution and the 2D images are used to assess areas, number or interactions between BBB components (Castejón, 2011; Cipolla et al., 2004; Haley and Lawrence, 2017). However, this technique is very time consuming and factors such as section folding or electron beam damage can lead to interrupted series and imperfect image stacks which may affect the interpretation of the results (Knott et al.,

2008). Automation protocols have significantly improved the efficiency of TEM image acquisition and processing, including image stacking and montage compilation, enabling the development of 3D reconstruction techniques based on TEM imaging (Mathiisen et al., 2010). This approach has several benefits over a 2D analysis, such as in-depth analysis of volume, localisation in space and analysis of 3D contact between several elements along the entirety of a reconstructed vessel. Therefore, the aim of this study was to analyse the ultrastructural changes in brain capillaries in the prefrontal cortex and CA1 region of the hippocampus of young and aged C57BL/6J female mice using 2D TEM images and 3D TEM reconstruction.

2. Material and Methods

2.1 Animals

6 and 24-month-old female C57BL/6J mice (3 animals per age group) were bred and housed at The Open University and kept on a 12-h light/dark cycle, with food and water provided *ad libitum*. Oestrous cycle was determined by vaginal lavage (0.2-0.4 mL of distilled water) at the start of the light phase for 7 consecutive days. All animals were sacrificed within the same 2-h period at the beginning of the light phase of the light/dark cycle. All animal experiments were handled in accordance and under the ethical approval of The Open University Animal Welfare and Ethics Research Board and the UK Home Office (PPL 80/2612).

2.2 Plasma collection and sex hormone measurement

Mice were injected with an overdose of pentobarbital sodium 20% w/v (Animalcare, York, UK) and blood was collected, spun down at 2000 g, 4 ^{o}C, for 3 min. Collected plasma was processed using ELISA to measure the concentrations of estradiol (Calbiotech, California, US) and progesterone (Crystal Chem, Zaandam, Netherlands), according to the manufacturers' instructions.

2.3 Brain collection and slicing

Mice were injected with an overdose of pentobarbital sodium 20% w/v (Animalcare, York, UK) and perfused intracardially with 0.01 M phosphate buffered saline (PBS), followed by 3% PFA and 1% glutaraldehyde in 0.1 M phosphate buffer (PB), pH 7.4. Brains were removed and kept in 2.5% glutaraldehyde in 0.1 M PB for 5 days. After this post-fixation time, brains were sliced coronally into slices of 50 µm thickness using a vibratome. Slices were stored in 0.1 M PB at 4ºC prior further processing.

2.4 TEM sample processing

Brain slices were transferred to fresh 2.5% glutaraldehyde (Agar Scientific, Essex, UK) in PB 0.1 M at RT for 1h, and then rinsed in 0.1 M PB. Afterwards, slices were incubated in 1% osmium tetroxide (Agar Scientific, Essex, UK) in 0.1 M PB for 1h at RT, followed by dehydration in increasing graded aqueous solutions of ethanol from 30% to 100%. After 100% ethanol, slices were incubated in 100% acetone followed by impregnation with a mixture of 50% Epon 812 epoxy resin (Sigma-Aldrich, Dorset, UK) and 50% pure acetone (50:50, resin:acetone) for 2h at RT. For resin embedding, slices were placed on top of a cleaned piece of aclar plastic film, pre-covered with resin:acetone mixture. Each slice was covered with a drop of pure resin and a second film of aclar was slowly placed on top, ensuring air bubbles were removed. Slices between both films were incubated at 60 ºC for 48h to promote resin polymerisation. Gelatine capsules filled with an identifying number and a drop of resin were also incubated at 60 ºC for 48h to polymerise. The slices were then uncovered, and the labelled capsules were placed on top of each one of them using pure resin before being incubated at 60 ºC for 48h. Each capsule was coded, and all further analyses were carried out with the investigator blind to the experimental status of the tissue. For serial sectioning, two capsules per animal (one for each brain region) were used. The slices located on the surface of each capsule were trimmed into a block of size 30 µm x 300 µm, which was serially sectioned into 50 nm sections by a diamond knife with a small metal boat attached to it and filled with water (Diatome, Switzerland). Ribbons of tissue sections were floated on the water and collected onto copper slot grids covered by a carbon coated pioloform film. Sections on the grids were left air drying for at least 2h.

For counter-staining, sections were pre-treated with 1% HCl for 1 min in order to reduce formation of crystals and then washed in distilled water. Sections were then stained with 3.5% aqueous uranyl acetate (Agar Scientific, Essex, UK) for 20 min and washed in distilled water. Finally, grids were stained with Reynold´s lead citrate (Delta Microscopies, Mauressac, France) for 7 min, washed in distilled water and left to air dry for at least 2h before imaging.

2.5 TEM imaging and 3D reconstruction

Selection of capillaries was based on the criteria of size (4-6 µm of diameter), presence of intact morphology, presence of pericyte processes and absence of vascular branching. Sections were imaged on a JEM 1400 electron microscope (Jeol, Tokyo, Japan). Images of selected capillaries were acquired automatically using an AMT XR60 camera (Deben, Suffolk, UK) and SerialEM software (https://bio3d.colorado.edu/SerialEM/), as described by Mastronarde (Mastronarde, 2005). Acquisition was performed using a column magnification of 6000x and acceleration voltage of 80 kV, and taking images of 3x4 frames (x: y axis) per section. Images were first corrected for projector lens distortion using the ImageJ plugin bUwarpJ (Arganda-carreras et al., 2006), and then stitched together into montages using Photomerge command in Adobe Photoshop CS6. For 3D reconstruction, montages were organised into serial stacks and automatically aligned using the ImageJ TrakEM2 plugin as described by Cardona (Cardona et al., 2012). From 1 to 2 stacks per capillary were analysed in each animal (~10 µm of total vessel length). Each stack included 50 to 100 montages. Capillaries were then reconstructed in 3D using Reconstruct software (http://synapseweb.clm.utexas.edu/software-0), by tracing the cellular and subcellular components of interest in each montage of a serial stack. Finally, generated 3D reconstructions of capillaries were smoothed, stylised and coloured using 3D Studio Max software (Autodesk, California, US). Reconstructed capillary segments showed total lengths of ~10 µm. The video of a fully 3D reconstructed vessel segment is shown in Supplementary Video 1.

2.6 Quantification and data collection

Structural features of interest including volumes, areas, numbers or lengths were quantified in the 3D reconstructed vessels using the tools provided by Reconstruct software. With regard to tight junctions, tortuosity was measured alongside the total vessel length taking three points (lumen, middle and BM sides of the junction) as reference in each section and obtaining a mean value. In addition, measurement of tight junction complexity was calculated by dividing the length of the tight junction by the diagonal of a rectangle containing the length and height of the whole tight junction, as explained previously by Jackman et al. (Jackman et al., 2013). Astrocyte – BM contact was calculated as the percentage of the surface area of the BM in direct contact with the astrocytic end-feet, using the flat surface values obtained in Reconstruct. Structures were traced within 2 µm from the point of astrocyte – BM contact, therefore it was not possible to identify an average number of astrocytic end-feet per capillary. Five different capillaries were analysed per animal in each brain region, and a mean value was calculated for each region in each animal (n=3 mice/age group).

2.7 Statistical analysis

All data is presented as mean ± SEM. GraphPad Prism 8.2.0 (La Jolla, USA) was used for statistical analysis. Shapiro-Wilk normality test and Q-Q plots were used to assess distribution of the data. Data from the preliminary study (2D and 3D cortex, and 3D hippocampus) was individually analysed by using two-tailed Student´s t-test, whereas two-way ANOVA and Sidak's correction test was used when comparing the data from the 3D analysis by region and age combined. In all cases the statistical significance was set at $p<0.05$.

3. Results

3.1 Structural 2D and 3D approaches differ when analysing features previously described to change with ageing.

Previous studies have shown that plasma oestrogen and progesterone concentrations in aged, reproductively senescent female C57BL/6 mice most closely matches hormone levels in the dioestrous phase of the oestrous cycle in young mice (Felicio et al., 1984; Nelson et al., 1981). In agreement with these previous studies, the progesterone to estradiol ratio (P:E2) did not show significant differences between young female mice in dioestrous and aged female mice (**Supplemental Fig. 1**). Therefore, to avoid potential effects of hormonal fluctuations on BBB structure that may confound interpretation of the data, oestrous cycle was monitored by vaginal lavage and all young females were confirmed to be in dioestrous on the day of tissue collection (**Supplemental Fig. 2**).

An initial comparison of analyses using 2D and 3D TEM images was performed by measuring three features of brain cortical capillaries previously described to change during ageing: BM thickness, BEC mitochondrial content and pericyte – BEC contact (**Fig. 1**). BM thickness was shown to be significantly increased in aged capillaries when compared to young capillaries in both 2D and 3D analyses (**Fig. 1A**). Interestingly, the other two features showed differences depending on the analysis performed. The number and volume of BEC mitochondria was significantly decreased in aged capillaries compared to young animals in the 2D analysis (**Fig. 1B**). However, the 3D analysis showed a significant decrease in the number but not volume of mitochondria in the aged cortical capillaries (**Fig. 1B**). Pericytic projections were observed to spread intermittently over the BECs. The percentage of pericyte coverage of the BECs did not differ between young and aged mice in the 2D analysis, although it was significantly increased in aged capillaries in the 3D analysis (**Fig. 1C**).

3.2 Regional differences between capillaries in young and aged mice using 3D reconstructed vessels when analysing features previously described to change with ageing.

According to these results, the 3D analysis appears to give more detailed information regarding volumes and cell-cell interactions. Therefore, additional analyses of cortical and hippocampal vessels were carried out using 3D reconstructed vessels. As shown for cortical capillaries in subsection 3.1, BM thickness, BEC mitochondrial content and pericyte – BEC contact were also measured in capillaries from the hippocampus **(Fig. 2)**. Hippocampal capillaries from aged mice showed a significantly thicker BM compared to young mice **(Fig. 2A)**. In contrast, and despite a tendency to increase, no changes in BEC mitochondrial number and volume or pericyte – BEC contact were observed in aged capillaries **(Fig. 2B and C)**. Comparisons of BM thickness, BEC mitochondrial content and pericyte – BEC contact in cortex and hippocampus of young and aged mice are summarised in **Table 1**. No significant regional differences were observed between cortical and hippocampal capillaries at any age in any of these features.

3.3 Morphological features in cortical and hippocampal BECs: BEC pseudopods and tight junctions.

When comparing young versus aged capillaries, filamentous pseudopod-like structures were observed to protrude from the endothelial cells into the lumen. According to the 3D analysis results, the number and volume of pseudopods was significantly higher in aged cortical endothelial cells compared to those in young cortical endothelial cells (**Fig. 3A and B**). No changes in pseudopod number or volume were observed in old versus young hippocampal capillaries (**Fig. 3A and B**). Regional comparisons found significantly more pseudopods and greater pseudopod volume in aged cortical capillaries compared to aged hippocampal capillaries (**Fig. 3A and B**).

In the 3D reconstructed capillaries, tight junctions were visible wherever two endothelial cells overlapped (**Fig. 4**). Analysis of tight junction tortuosity was performed along the longitudinal length

of the capillary as an average of three reference points in the lumen, middle and basement membrane sides of the tight junction (**Fig. 4A**). Aged cortical capillaries showed a significantly greater degree of tight junction tortuosity compared to cortical young capillaries (**Fig. 4B**). In contrast, hippocampal capillaries did not show any significant changes in tight junction tortuosity due to ageing (**Fig. 4B**). However, when comparing aged capillaries of both regions, aged cortical capillaries showed higher tight junction tortuosity than aged hippocampal capillaries. Measurement of tight junction complexity was performed as published by Jackman and colleagues as transverse length (Jackman et al., 2013) (**Fig. 5A**), and showed no significant differences when comparing young and aged capillaries in any region (**Fig. 5B**). However, when comparing aged capillaries from both regions, tight junction complexity was found to be significantly lower in cortical capillaries (**Fig. 5B**).

3.4 Morphological features in pericytes and astrocytes from cortex and hippocampus: pericyte mitochondria and astrocytic end-feet coverage.

As assessed for BEC mitochondria in subsection 3.1, the number and volume of pericytic mitochondria were measured in 3D reconstructed cortical and hippocampal capillaries. The number of mitochondria contained within pericytes did not differ between young and aged mice in either the cortex or hippocampus (**Fig. 6A**). By contrast, pericyte mitochondrial volume was significantly higher in aged capillaries of both cortex and hippocampus compared to younger animals (**Fig. 6B**). Additionally, it was also noted that in some cases mitochondria of aged pericytes formed tubular networks. No significant changes were observed between regions in animals of any age.

In 3D reconstructed capillaries, astrocytic end-feet were found to ensheath the vessel, in intimate contact with the surrounding BM (**Fig. 7**). The percentage of astrocyte coverage of the BM did not show any significant age-related changes in capillaries of cortex or hippocampus. Similarly, no significant differences were observed in astrocyte end-feet coverage between cortical and hippocampal capillaries at any age (**Fig. 7**).

4. Discussion

The present study confirms that the female BBB changes with age and shows age-related alterations similar to those previously described in the literature, including increased BM thickness, changes in BEC mitochondrial component and altered pericyte – BEC contact. Modifications in BEC surface, tight junction tortuosity and complexity and pericytic mitochondria were also observed in brain capillaries of aged female mice. Regional comparisons indicated more changes in aged capillaries in the prefrontal cortex compared to those in the hippocampus.

The vast majority of ultrastructural studies on the effects of ageing at the BBB have been carried out using 2D analyses despite technical limitations which may affect the interpretation of the results (Knott et al., 2008). Therefore, we first carried out a comparison between analyses done on 2D images and 3D reconstructed models obtained by TEM from cortical capillaries. Despite some features being similarly changed when assessed by either technique (e.g. BM thickness), other measurements did not correlate between analyses (e.g. BEC mitochondrial content or pericyte – BEC coverage). This discrepancy might be due to the different resolutions available using each method. For example, the lack of depth in the 2D analysis might limit the measurement of certain structures or lead to misinterpretation. Additional depth information obtained from the 3D reconstruction, allows for the identification of features that are not as visible in flat images (e.g. changes in pericyte coverage) or give a different perspective depending on the feature (e.g. tubular mitochondria), which become useful when analysing complex and interrelated structures in brain microvessels (Mathiisen et al., 2010). Therefore, 3D reconstructed capillaries were chosen to carry out additional analyses of BBB characteristics between young and aged animals and between brain regions.

Ultrastructural changes affecting cellular and subcellular components of the BBB, including pericytes, BM and TJ proteins, may be associated with detrimental effects on blood perfusion and metabolite clearance mechanisms in the cerebral vasculature, which may also contribute to cognitive decline and neurodegeneration (Ito et al., 2013; Morris et al., 2014; Sweeney et al., 2016). Among the observed age-related changes in BBB subcellular composition, a thicker BM in ageing is in agreement with recent studies in male mice that showed BM thickness to be doubled in aged cortical and

hippocampal microvessels (Ceafalan et al., 2019). This increase in thickness has also been observed in other species including human and rat during normal ageing, as well as in association with neurodegenerative diseases in both men and women (Alba et al., 2004; Farkas et al., 2006; Hicks et al., 1983; Morris et al., 2014). The higher BM thickness and stiffness observed in ageing has previously been correlated with changes in the proportion of extracellular matrix proteins such as collagen IV and laminins (Candiello et al., 2010; Ceafalan et al., 2019; Uspenskaia et al., 2004), leading to altered cerebral blood flow, accumulation of unwanted proteins and hindered clearance mechanisms in the mouse cerebrovasculature (Hawkes et al., 2011). Altogether, these results suggest that BM thickening is a universal feature in the ageing cerebrovasculature, and it may contribute to and exacerbate several neurodegenerative disorders that have a vascular component.

Mitochondrial changes have also been described in the ageing BBB of mice, non-human primates and humans, and are commonly associated with oxidative stress and pro-inflammatory processes in the cerebral cortex (Burns et al., 1979; Enciu et al., 2013; Sure et al., 2018). Mitochondrial morphology is linked to its function, and depends on the balance of fusion and fission mechanisms (Aerts et al., 2008; Leadsham and Gourlay, 2010), which have been observed to change in ageing, leading to alterations in shape or accumulation of mitochondrial damage (Jendrach et al., 2005; Scheckhuber et al., 2011). The age-related loss of BEC mitochondria observed in the present study is in agreement with several studies that described a decrease in mitochondrial number and volume in BECs of aged male rodents and non-human primates and human endothelial cells *in vitro* (Burns et al., 1979; Hicks et al., 1983; Jendrach et al., 2005). In addition, changes in mitochondrial shape have also been linked to mitophagy in ageing (Sun et al., 2015), in which either increased mitochondrial fission events lead to senescence and cell death (Scheckhuber et al., 2011), or, by contrast, reduced fission activity and development of network-like morphology postpones mitochondrial dysfunction and ageing, thereby promoting maintenance of cell viability (Gomes et al., 2011). Our results suggest that BEC and pericyte mitochondria are differently affected by senescence. Given that the BBB has a high metabolic demand and mitochondria are related to cell physiology (Haddad-Tóvolli et al., 2017), modifications in their morphology might enhance the higher sensitivity

of the BBB to oxidant stressors, which together with decreased expression of antioxidant proteins and increased presence of reactive oxygen species in ageing, might promote cerebrovasculature damage (Grammas et al., 2011). Our observation of tubular networks of mitochondria in aged pericytes suggests that pericytes might be more resistant to age-induced damage than BECs in the female BBB. Interestingly, sex-specific differences have been reported in mitochondrial fission/fusion balance of cultured mouse cortical astrocytes, with female astrocytes having a higher level of mitochondrial fusion and therefore increased cell viability, an effect described to be mainly mediated by oestrogen (Arnold et al., 2008). Although astrocytic mitochondria were not measured in the present study, these findings suggest that a similar effect might be happening in female pericytes, and, when reproductive senescence strikes and sex hormone levels change, the mitochondrial component may promote cell viability in pericytes but not in BECs. Further studies on cell viability and mitochondrial activity might help to confirm and to better understand whether these structural alterations are related to changes in mitochondrial and cellular function.

In addition to changes in mitochondrial content, BEC luminal surface projections, or pseudopods, were observed to vary in size and number during ageing, when analysed by 3D reconstruction in the cortex only. These results are consistent with previous studies that showed large luminal projections on BECs of senescence-accelerated mice, although this same study described them in hippocampal vessels and no quantitative analysis was carried out (Lee et al., 2000). BEC pseudopod-like microstructures have also been reported under inflammatory conditions in injured mouse BBB during encephalomyelitis (Lossinsky et al., 1991), and more recently in cultured human microvessel endothelial cells stimulated with chemokines such as CCL5 (Whittall et al., 2013). Also, recent *in vitro* studies with human endothelial cells, stimulated with tumour necrosis factor-α and interferon-γ, have shown surface structures that can be compared to these pseudopods, and also express and present adhesion molecules and chemokines (Øynebråten et al., 2015). Together, these findings suggest that higher number and volume of pseudopods in the ageing female BBB may increase the interaction of BECs with immune cells under pro-inflammatory conditions. A higher pro-inflammatory state in the female BBB during ageing is supported by previous studies that found a

greater upregulation of genes related to immune activation and inflammation in the aged female brain compared to the aged male brain (Berchtold et al., 2008). BEC tight junctions have also been described to change during ageing, mainly related to BBB dysfunction in male rodents (Goodall et al., 2018; Mooradian et al., 2003). We assessed tight junction morphology by measuring both complexity and tortuosity. Reduced tight junction complexity has been linked to BBB disruption in granulin mutant male mice after ischemic stroke (Jackman et al., 2013), while changes in tight junction morphology in blood vessels of human glioblastoma have been shown to correlate with abnormal junctional protein expression and distribution (Liebner et al., 2000a). Correspondingly, decreased tight junction protein expression has also been observed in human cortical endothelial cells during the progression of Alzheimer´s disease (Yamazaki et al., 2019). Also, increased tortuosity of tight junctions has been shown in post-capillary venules in the spinal cord of EAE mice when compared to vessels in healthy animals, which may lead to alterations in barrier permeability and immune cell transmigration into the brain (Lutz et al., 2017). Therefore, as mentioned above for BEC pseudopods, the higher tight junction tortuosity observed at the female neurovasculature in our study might be related to an age-dependent increase in neuroinflammation. Previous studies have reported that ovariectomisation of middle-aged female rats lead to age-related loss of tight junction proteins depending on the brain region, in association with altered paracellular permeability in hippocampus (Bake et al., 2009; Bake and Sohrabji, 2004), but not in cortex (Sandoval and Witt, 2011). In these studies, changes in estradiol concentration were associated with regulation of BBB permeability. Altogether, these observations suggest that both tight junction organisation and morphology and their effect on permeability may be differentially regulated between brain regions, which might correlate to loss of sex steroid hormones and an enhanced neuroinflammatory state during reproductive senescence.

Another important aspect of BBB function is the interaction between its different cellular and subcellular components. Pericytes play an important role in vessel stabilisation, BEC proliferation and modulation of capillary blood flow (Armulik et al., 2005; Cai et al., 2018; Ramsauer et al., 2002). Pericytes cover abluminal surface of BECs and share the same BM (Banerjee and Bhat, 2007;

Hellström et al., 1999), which allows a crosstalk between both cell types (Darland et al., 2003; Ribatti et al., 2011), that is enhanced in the so-called peg-and-socket interdigitations, where gap and adherens junctions promote close interconnection and exchange of nutrients, metabolites or ions (Li et al., 2011; Liu et al., 2012; Winkler et al., 2011). In addition, BEC – pericyte contact has been shown to induce junctional protein expression and BBB formation, integrity and maintenance (Dohgu et al., 2005; Shimizu et al., 2008). BECs and pericytes also interact with astrocytes, mediating attachment of the astrocytic end-feet and promoting a virtually complete ensheathment of the vessel (Armulik et al., 2010; Mathiisen et al., 2010). Astrocytes have also been proved to promote BBB formation and maintenance in humans and rodents by inducing expression of tight junction proteins such as claudin-5 or zonula occludens-1, as well as redistribution and polarized localisation of BEC transporters (Abbott et al., 2006; Al Ahmad et al., 2011; Obermeier et al., 2013). Both pericyte and astrocyte contacts have been reported to be decreased in male rodents during ageing, which leads to BBB breakdown and neurovascular dysfunction (Duncombe et al., 2017; Hughes et al., 2006). Our findings are in contrast with previous reports that showed either no change in pericyte coverage in aged male rodents (Bors et al., 2018; Goodall et al., 2018), or a significant decrease in both aged male (Bell et al., 2010) and female mice (Soto et al., 2015). Although more experiments are needed to determine the factors that contribute to these discrepancies, they may relate to technical differences between the analyses carried out using 2D images in the previous experiments and the 3D analysis performed in the current study, in addition to some difficulties in measuring pericyte projections. Similarly, the lack of significant age-related changes in astrocyte coverage in capillaries of any region is not consistent with previous studies that reported decreased astrocyte coverage over brain microvessels in male mice (Duncombe et al., 2017). Interestingly, astrocyte number has been reported to be higher in aged female mice compared to young female mice and aged male mice (Mouton et al., 2002), suggesting potential sex differences in both baseline astrocyte density and their response to age and changes in sex hormone concentrations. Indeed, sex-dependent increase in astrocyte number, in addition to the above-mentioned astrocyte increased viability due to higher levels of mitochondrial fusion (Arnold et al., 2008), might attenuate the ageing effect on astrocytic end-feet coverage in the female BBB. These findings, together with several other reports cited in this discussion, suggest that the BBB components

might age differently in females when compared to males. The absence of males in the present study hinders an in-depth assessment of potential sex-dependent alterations in brain capillary ultrastructure. The inclusion of males in a future comparative analysis would help identifying possible factors based on sex specificity that may correlate to the structural alterations observed in the ageing female BBB.

In addition to age-dependent alterations, the present study showed regional differences between prefrontal cortex and hippocampus. The BBB of cortical capillaries appeared to undergo more age-related ultrastructural alterations than that of hippocampal capillaries. Although previous studies have reported a sensitivity of hippocampal vessels to ageing (Lee et al., 2000; Lourenço et al., 2018; Topple et al., 1991), a recent study in aged male mice has shown cortical blood vessels to be more strongly affected by cholinergic denervation than those in hippocampus (Nizari et al., 2019), which might have important consequences in age-related vasculopathies including BBB disruption. Further comparisons of BBB changes between brain regions, and between males and females, would help understanding the role of these structural changes on BBB function and whether sex specificity is also contributing to the regional differences.

5. Conclusion

The present study provides evidence of the female BBB being altered at the ultrastructural level during normal ageing. Collectively, our results indicate age-related structural changes in the BBB of female mice that affect BM thickness, mitochondrial morphology, BEC surface and tight junctions and cell-cell contacts. Such changes might be associated with functional alterations in barrier permeability, capillary blood flow, inflammation, energy production and oxidative stress. Therefore, studies looking into inflammatory signals, pericyte viability, mitochondrial function and specific tight junction protein expression and distribution at the aged female BBB, may shed new light onto the described ultrastructural changes and the real extent of their impact on cerebrovascular function. These alterations may also contribute to the specific sex differences observed regarding incidence and progression of cerebrovascular diseases between males and females, as well as the

development of certain age-induced neurodegenerative disorders that present a vascular component and appear to be more prevalent in post-menopausal women.

Acknowledgements

Funding: this work was supported by the European Commission under a Marie Sklodowska-Curie Innovative Training Network: BtRAIN – European Brain Barriers Training Network (H2020-MSCA-ITN-2015, nº 675619) and by the Open University. The Open University is incorporated by Royal Charter (RC 000391), an exempt charity in England and Wales and a charity registered in Scotland (SC 038302). The Open University is authorized and regulated by the Financial Conduct Authority. We would like to express our gratitude to Karen Evans, Agata Stramek and Iwona Loza from the Biomedical Research Unit at the Open University, for their help in animal husbandry. We would also like to thank Core facilities of Pushchino Centre of Biological Research for letting VR use their equipment to improve our TEM protocol.

Disclosure statement

All the authors have seen and approved the manuscript, there are no financial or personal conflicts of interest related to this work.

Author contributions

EFA, IAR and CAH conceived the experiments. EFA performed the experiments, data analysis, and manuscript preparation and editing. IK, RG and VR assisted with the TEM methodology and analysis. DKM and FC assisted with data analysis and interpretation.

References

Abbott, N.J., Rönnbäck, L., Hansson, E., 2006. Astrocyte–endothelial interactions at the blood–brain barrier. Nat. Rev. Neurosci. 7, 41–53. https://doi.org/10.1038/nrn1824

Aerts, A.M., Zabrocki, P., François, I.E.J.A., Carmona-Gutierrez, D., Govaert, G., Mao, C., Smets, B., Madeo, F., Winderickx, J., Cammue, B.P.A., Thevissen, K., 2008. Ydc1p ceramidase triggers organelle fragmentation, apoptosis and accelerated ageing in yeast. Cell. Mol. Life Sci. 65, 1933–1942. https://doi.org/10.1007/s00018-008-8129-8

Al Ahmad, A., Taboada, C.B., Gassmann, M., Ogunshola, O.O., 2011. Astrocytes and pericytes differentially modulate blood-brain barrier characteristics during development and hypoxic insult. J. Cereb. Blood Flow Metab. 31, 693–705. https://doi.org/10.1038/jcbfm.2010.148

Alba, C., Vidal, L., Díaz, F., Villena, A., Vargas, I.P. De, 2004. Ultrastructural and quantitative age-related changes in capillaries of the dorsal lateral geniculate nucleus. Brain Res. Bull. 64, 145–153. https://doi.org/10.1016/j.brainresbull.2004.06.006

Altmann, A., Tian, L., Henderson, V.W., Greicius, M.D., 2014. Sex modifies the APOE-related risk of developing Alzheimer disease. Ann. Neurol. 75, 563–573. https://doi.org/10.1002/ana.24135

Amenta, F., Bronzetti, E., Sabbatini, M., Vega, J.A., 1998. Astrocyte changes in aging cerebral cortex and hippocampus: A quantitative immunohistochemical study. Microsc. Res. Tech. 43, 29–33. https://doi.org/10.1002/(SICI)1097-0029(19981001)43:1<29::AID-JEMT5>3.0.CO;2-H

Arganda-carreras, I., Sorzano, C.O.S., Marabini, R., Carazo, M., Ortiz-de-solórzano, C., Kybic, J., 2006. Consistent and Elastic Registration of Histological Sections using Vector-Spline Regularization. Lect. Notes Comput. Sci. 4241, 85–95.

Armulik, A., Abramsson, A., Betsholtz, C., 2005. Endothelial / Pericyte Interactions. Circ. Res. 97, 512–523. https://doi.org/10.1161/01.RES.0000182903.16652.d7

Armulik, A., Genové, G., Mäe, M., Nisancioglu, M.H., Wallgard, E., Niaudet, C., He, L., Norlin, J., Lindblom, P., Strittmatter, K., Johansson, B.R., Betsholtz, C., 2010. Pericytes regulate the blood-brain barrier. Nature 468, 557–561. https://doi.org/10.1038/nature09522

Arnold, S., de Araújo, G.W., Beyer, C., 2008. Gender-specific regulation of mitochondrial fusion and fission gene transcription and viability of cortical astrocytes by steroid hormones. J. Mol. Endocrinol. 41, 289–

300. https://doi.org/10.1677/JME-08-0085

Bake, S., Friedman, J.A., Sohrabji, F., 2009. Reproductive age-related changes in the blood brain barrier: Expression of IgG and tight junction proteins. Microvasc. Res. 78, 413–424. https://doi.org/10.1016/j.mvr.2009.06.009

Bake, S., Sohrabji, F., 2004. 17B-Estradiol Differentially Regulates Blood-Brain Barrier Permeability in Young and Aging Female Rats. Endocrinology 145, 5471–5475. https://doi.org/10.1210/en.2004-0984

Banerjee, S., Bhat, M.A., 2007. Neuron-Glial Interactions in Blood-Brain Barrier Formation. Annu. Rev. Neurosci. 30, 235–258. https://doi.org/10.1146/annurev.neuro.30.051606.094345

Begley, D.J., 2004. ABC Transporters and the blood-brain barrier. Curr. Pharm. Des. 10, 1295–1312.

Bell, R.D., Winkler, E.A., Sagare, A.P., Singh, I., LaRue, B., Deane, R., Zlokovic, B. V., 2010. Pericytes Control Key Neurovascular Functions and Neuronal Phenotype in the Adult Brain and during Brain Aging. Neuron 68, 409–427. https://doi.org/10.1016/j.neuron.2010.09.043

Berchtold, N.C., Cribbs, D.H., Coleman, P.D., Rogers, J., Head, E., Kim, R., Beach, T., Miller, C., Troncoso, J., Trojanowski, J.Q., Zielke, H.R., Cotman, C.W., 2008. Gene expression changes in the course of normal brain aging are sexually dimorphic. Proc. Natl. Acad. Sci. U. S. A. 105, 15605–15610. https://doi.org/10.1073/pnas.0806883105

Bors, L., Tóth, K., Tóth, E.Z., Bajza, Á., Csorba, A., Szigeti, K., Máthé, D., Perlaki, G., Orsi, G., Tóth, G.K., Erdő, F., 2018. Age-dependent changes at the blood-brain barrier. A Comparative structural and functional study in young adult and middle aged rats. Brain Res. Bull. 139, 269–277. https://doi.org/10.1016/j.brainresbull.2018.03.001

Burns, E.M., Kruckeberg, T.W., Comerford, L.E., Buschman, M.T., 1979. Thinning of capillary walls and declining numbers of endothelial mitochondria in the cerebral cortex of the aging primate, Macaca nemestrina. Journals Gerontol. 34, 642–650. https://doi.org/10.1093/geronj/34.5.642

Cai, C., Fordsmann, J.C., Jensen, S.H., Gesslein, B., Lønstrup, M., Hald, B.O., Zambach, S.A., Brodin, B., Lauritzen, M.J., 2018. Stimulation-induced increases in cerebral blood flow and local capillary vasoconstriction depend on conducted vascular responses. Proc. Natl. Acad. Sci. U. S. A. 115, E5796–E5804. https://doi.org/10.1073/pnas.1707702115

Candiello, J., Cole, G.J., Halfter, W., 2010. Age-dependent changes in the structure, composition and

biophysical properties of a human basement membrane. Matrix Biol. 29, 402–410. https://doi.org/10.1016/j.matbio.2010.03.004

Cardona, A., Saalfeld, S., Schindelin, J., Arganda-carreras, I., Preibisch, S., Longair, M., Tomancak, P., Hartenstein, V., Douglas, R.J., 2012. TrakEM2 Software for Neural Circuit Reconstruction 7. https://doi.org/10.1371/journal.pone.0038011

Castejón, O.J., 2011. Ultrastructural pathology of cortical capillary pericytes in human traumatic brain oedema. Folia Neuropathol. 49, 162–173.

Ceafalan, L.C., Fertig, T.E., Gheorghe, T.C., Hinescu, M.E., Popescu, B.O., Pahnke, J., Gherghiceanu, M., 2019. Age-related ultrastructural changes of the basement membrane in the mouse blood- brain barrier. J. Cell. Mol. Med. 819–827. https://doi.org/10.1111/jcmm.13980

Cipolla, M.J., Crete, R., Vitullo, L., Rix, R.D., 2004. Transcellular Transport as a mechanism of blood-brain barrier disruption during stroke. Front. Biosci. 9, 777–785.

Corcoran, M.P., Meydani, M., Lichtenstein, A.H., Schaefer, E.J., Lamon-fava, S., 2010. Sex hormone modulation of proinflammatory cytokine and CRP expression in macrophages from older men and postmenopausal women 206, 217–224. https://doi.org/10.1677/JOE-10-0057.Sex

Cullen, K.M., Kócsi, Z., Stone, J., 2005. Pericapillary haem-rich deposits: Evidence for microhaemorrhages in aging human cerebral cortex. J. Cereb. Blood Flow Metab. 25, 1656–1667. https://doi.org/10.1038/sj.jcbfm.9600155

Darland, D.C., Massingham, L.J., Smith, S.R., Piek, E., Saint-Geniez, M., D'Amore, P.A., 2003. Pericyte production of cell-associated VEGF is differentiation-dependent and is associated with endothelial survival. Dev. Biol. 264, 275–288. https://doi.org/10.1016/j.ydbio.2003.08.015

Dohgu, S., Takata, F., Yamauchi, A., Nakagawa, S., Egawa, T., Naito, M., Tsuruo, T., Sawada, Y., Niwa, M., Kataoka, Y., 2005. Brain pericytes contribute to the induction and up-regulation of blood-brain barrier functions through transforming growth factor-β production. Brain Res. 1038, 208–215. https://doi.org/10.1016/j.brainres.2005.01.027

Duncombe, J., Lennen, R.J., Jansen, M.A., Marshall, I., Wardlaw, J.M., Horsburgh, K., 2017. Ageing causes prominent neurovascular dysfunction associated with loss of astrocytic contacts and gliosis. Neuropathol. Appl. Neurobiol. 43, 477–491. https://doi.org/10.1111/nan.12375

Elahy, M., Jackaman, C., Mamo, J.C., Lam, V., Dhaliwal, S.S., Giles, C., Nelson, D., Takechi, R., 2015. Blood-brain barrier dysfunction developed during normal aging is associated with inflammation and loss of tight junctions but not with leukocyte recruitment. Immun. Ageing 12, 2. https://doi.org/10.1186/s12979-015-0029-9

Enciu, A.M., Gherghiceanu, M., Popescu, B.O., 2013. Triggers and effectors of oxidative stress at blood-brain barrier level: Relevance for brain ageing and neurodegeneration. Oxid. Med. Cell. Longev. 2013. https://doi.org/10.1155/2013/297512

Farkas, E., de Vos, R.A.I., Donka, G., Jansen Steur, E.N., Mihály, A., Luiten, P.G.M., 2006. Age-related microvascular degeneration in the human cerebral periventricular white matter. Acta Neuropathol. 111, 150–157. https://doi.org/10.1007/s00401-005-0007-y

Farrell, C.R., Stewart, P.A., Farrell, C.L., Del Maestro, R.F., 1987. Pericytes in human cerebral microvasculature. Anat. Rec. 218, 466–469. https://doi.org/10.1002/ar.1092180416

Felicio, L.S., Nelson, J.F., Finch, C.E., 1984. Longitudinal Studies of Estrous Cyclicity in Aging C57BL/6J Mice: II. Cessation of Cyclicity and the Duration of Persistent Vaginal Cornification 1. Biol. Reprod. 31, 446–453. https://doi.org/10.1095/biolreprod31.3.446

Gavin, K.M., Seals, D.R., Silver, A.E., Moreau, K.L., 2009. Vascular endothelial estrogen receptor α is modulated by estrogen status and related to endothelial function and endothelial nitric oxide synthase in healthy women. J. Clin. Endocrinol. Metab. 94, 3513–3520. https://doi.org/10.1210/jc.2009-0278

Gee, J.R., Keller, J.N., 2005. Astrocytes: Regulation of brain homeostasis via apolipoprotein E. Int. J. Biochem. Cell Biol. 37, 1145–1150. https://doi.org/10.1016/j.biocel.2004.10.004

Gomes, L.C., Benedetto, G. Di, Scorrano, L., 2011. During autophagy mitochondria elongate, are spared from degradation and sustain cell viability. Nat. Cell Biol. 13, 589–598. https://doi.org/10.1038/ncb2220

Goodall, E.F., Wang, C., Simpson, J.E., Baker, D.J., Drew, D.R., Heath, P.R., Saffrey, M.J., Romero, I.A., Wharton, S.B., 2018. Age-associated changes in the blood-brain barrier: comparative studies in human and mouse. Neuropathol. Appl. Neurobiol. 44, 328–340. https://doi.org/10.1111/nan.12408

Grammas, P., Martinez, J., Miller, B., 2011. Cerebral microvascular endothelium and the pathogenesis of neurodegenerative diseases. Expert Rev. Mol. Med. 13, 1–22. https://doi.org/10.1017/S1462399411001918

Haddad-Tóvolli, R., Dragano, N.R.V., Ramalho, A.F.S., Velloso, L.A., 2017. Development and function of the blood-brain barrier in the context of metabolic control. Front. Neurosci. 11, 1–12. https://doi.org/10.3389/fnins.2017.00224

Haley, M.J., Lawrence, C.B., 2017. The blood-brain barrier after stroke: Structural studies and the role of transcytotic vesicles. J. Cereb. Blood Flow Metab. 37, 456–470. https://doi.org/10.1177/0271678X16629976

Hawkes, C.A., Härtig, W., Kacza, J., Schliebs, R., Weller, R.O., Nicoll, J.A., Carare, R.O., 2011. Perivascular drainage of solutes is impaired in the ageing mouse brain and in the presence of cerebral amyloid angiopathy. Acta Neuropathol. 121, 431–443. https://doi.org/10.1007/s00401-011-0801-7

He, J., Evans, C.O., Hoffman, S.W., Oyesiku, N.M., Stein, D.G., 2004. Progesterone and allopregnanolone reduce inflammatory cytokines after traumatic brain injury. Exp. Neurol. 189, 404–412. https://doi.org/10.1016/j.expneurol.2004.06.008

Hellström, M., Kalén, M., Lindahl, P., Abramsson, A., Betsholtz, C., 1999. Role of PDGF-B and PDGFR-β in recruitment of vascular smooth muscle cells and pericytes during embryonic blood vessel formation in the mouse. Development 126, 3047–3055.

Hicks, P., Rolsten, C., Brizzee, D., Samorajski, T., 1983. Age-related changes in rat brain capillaries. Neurobiol. Aging 4, 69–75. https://doi.org/10.1016/0197-4580(83)90057-X

Hughes, S., Gardiner, T., Hu, P., Baxter, L., Rosinova, E., Chan-Ling, T., 2006. Altered pericyte-endothelial relations in the rat retina during aging: Implications for vessel stability. Neurobiol. Aging 27, 1838–1847. https://doi.org/10.1016/j.neurobiolaging.2005.10.021

Ishrat, T., Sayeed, I., Atif, F., Hua, F., Stein, D.G., 2010. Progesterone and allopregnanolone attenuate blood-brain barrier dysfunction following permanent focal ischemia by regulating the expression of matrix metalloproteinases. Exp. Neurol. 226, 183–190. https://doi.org/10.1016/j.expneurol.2010.08.023

Ito, S., Matsumiya, K., Ohtsuki, S., Kamiie, J., Terasaki, T., 2013. Contributions of degradation and brain-to-blood elimination across the blood-brain barrier to cerebral clearance of human amyloid-β peptide(1-40) in mouse brain. J. Cereb. Blood Flow Metab. 33, 1770–1777. https://doi.org/10.1038/jcbfm.2013.125

Jackman, K., Kahles, T., Lane, D., Garcia-Bonilla, L., Abe, T., Capone, C., Hochrainer, K., Voss, H., Zhou, P., Ding, A., Anrather, J., Iadecola, C., 2013. Progranulin Deficiency Promotes Post-Ischemic Blood-Brain

Barrier Disruption. J. Neurosci. 33, 19579–19589. https://doi.org/10.1523/jneurosci.4318-13.2013

Jendrach, M., Pohl, S., Vöth, M., Kowald, A., Hammerstein, P., Bereiter-Hahn, J., 2005. Morpho-dynamic changes of mitochondria during ageing of human endothelial cells. Mech. Ageing Dev. 126, 813–821. https://doi.org/10.1016/j.mad.2005.03.002

Kanaan, N.M., Kordower, J.H., Collier, T.J., 2010. Age-related changes in glial cells of dopamine midbrain subregions in rhesus monkeys. Neurobiol Aging 31, 937–952. https://doi.org/10.1038/jid.2014.371

Kastin, A.J., Akerstrom, V., Maness, L.M., 2001. Chronic loss of ovarian function decreases transport of leptin into mouse brain. Neurosci. Lett. 310, 69–71. https://doi.org/10.1016/S0304-3940(01)02074-2

Knott, G., Marchman, H., Wall, D., Lich, B., 2008. Serial Section Scanning Electron Microscopy of Adult Brain Tissue Using Focused Ion Beam Milling. J. Neurosci. 28, 2959–2964. https://doi.org/10.1523/jneurosci.3189-07.2008

Krause, D.N., Duckles, S.P., Pelligrino, D.A., 2006. Influence of sex steroid hormones on cerebrovascular function. J. Appl. Physiol. 101, 1252–1261. https://doi.org/10.1152/japplphysiol.01095.2005

Leadsham, J.E., Gourlay, C.W., 2010. CAMP/PKA signaling balances respiratory activity with mitochondria dependent apoptosis via transcriptional regulation. BMC Cell Biol. 11. https://doi.org/10.1186/1471-2121-11-92

Lee, E.Y., Lee, S.Y., Lee, T.S., Chi, J.G., Choi, W., Suh, Y.H., 2000. Ultrastructural changes in microvessel with age in the hippocampus of senescence-accelerated mouse (sam)-p/10. Exp. Aging Res. 26, 3–14. https://doi.org/10.1080/036107300243650

Li, F., Lan, Y., Wang, Youliang, Wang, J., Yang, G., Meng, F., Han, H., Meng, A., Wang, Yaping, Yang, X., 2011. Endothelial Smad4 Maintains Cerebrovascular Integrity by Activating N-Cadherin through Cooperation with Notch. Dev. Cell 20, 291–302. https://doi.org/10.1016/j.devcel.2011.01.011

Liebner, S., Fischmann, A., Rascher, G., Duffner, F., Grote, E.-H., Kalbacher, H., Wolburg, H., 2000a. Claudin-1 and claudin-5 expression and tight junction morphology are altered in blood vessels of human glioblastoma multiforme. Acta Neuropathol. 323–331.

Liebner, S., Kniesel, U., Kalbacher, H., Wolburg, H., 2000b. Correlation of tight junction morphology with the expression of tight junction proteins in blood-brain barrier endothelial cells. Eur. J. Cell Biol. 79, 707–717. https://doi.org/10.1078/0171-9335-00101

Liu, S., Agalliu, D., Yu, C., Fisher, M., 2012. The Role of Pericytes in Blood-Brain Barrier Function and Stroke. Curr. Pharm. Des. 18, 3653–3662. https://doi.org/10.2174/138161212802002706

Lossinsky, A.S., Pluta, R., Song, M.J., Badmajew, V., Moretz, R.C., Wisniewski, H.M., 1991. Mechanisms of inflammatory cell attachment in chronic relapsing experimental allergic encephalomyelitis: A scanning and high-voltage electron microscopic study of the injured mouse blood-brain barrier. Microvasc. Res. 41, 299–310. https://doi.org/10.1016/0026-2862(91)90030-F

Lourenço, C.F., Ledo, A., Caetano, M., Barbosa, R.M., Laranjinha, J., 2018. Age-dependent impairment of neurovascular and neurometabolic coupling in the hippocampus. Front. Physiol. 9, 1–11. https://doi.org/10.3389/fphys.2018.00913

Lutz, S.E., Smith, J.R., Kim, D.H., Olson, C.V.L., Ellefsen, K., Bates, J.M., Gandhi, S.P., Agalliu, D., 2017. Caveolin1 Is Required for Th1 Cell Infiltration, but Not Tight Junction Remodeling, at the Blood-Brain Barrier in Autoimmune Neuroinflammation. Cell Rep. 21, 2104–2117. https://doi.org/10.1016/j.celrep.2017.10.094

Maggioli, E., McArthur, S., Mauro, C., Kieswich, J., Kusters, D.H.M., Reutelingsperger, C.P.M., Yaqoob, M., Solito, E., 2016. Estrogen protects the blood–brain barrier from inflammation-induced disruption and increased lymphocyte trafficking. Brain. Behav. Immun. 51, 212–222. https://doi.org/10.1016/j.bbi.2015.08.020

Mastronarde, D.N., 2005. Automated electron microscope tomography using robust prediction of specimen movements 152, 36–51. https://doi.org/10.1016/j.jsb.2005.07.007

Mathiisen, T.M., Lehre, K.P., Danbolt, N.C., Ottersen, O.P., 2010. The perivascular astroglial sheath provides a complete covering of the brain microvessels: An electron microscopic 3D reconstruction. Glia 58, 1094–1103. https://doi.org/10.1002/glia.20990

Montagne, A., Barnes, S.R., Sweeney, M.D., Halliday, M.R., Sagare, A.P., Zhao, Z., Toga, A.W., Jacobs, R.E., Liu, C.Y., Amezcua, L., Harrington, M.G., Chui, H.C., Law, M., Zlokovic, B. V., 2015. Blood-Brain barrier breakdown in the aging human hippocampus. Neuron 85, 296–302. https://doi.org/10.1016/j.neuron.2014.12.032

Mooradian, A.D., Haas, M.J., Chehade, J.M., 2003. Age-related changes in rat cerebral occludin and zonula occludens-1 (ZO-1). Mech. Ageing Dev. 124, 143–146. https://doi.org/10.1016/S0047-6374(02)00041-6

Morris, A.W.J., Carare, R.O., Schreiber, S., Hawkes, C.A., 2014. The cerebrovascular basement membrane: Role in the clearance of β-amyloid and cerebral amyloid angiopathy. Front. Aging Neurosci. 6, 1–9. https://doi.org/10.3389/fnagi.2014.00251

Mouton, P.R., Long, J.M., Lei, D.L., Howard, V., Jucker, M., Calhoun, M.E., Ingram, D.K., 2002. Age and gender effects on microglia and astrocyte numbers in brains of mice. Brain Res. 956, 30–35. https://doi.org/10.1016/S0006-8993(02)03475-3

Nelson, J.F., Felicio, L.S., Osterburg, H.H., Finch, C.E., 1981. Altered Profiles of Estradiol and Progesterone Associated with Prolonged Estrous Cycles and Persistent Vaginal Cornification in Aging C578L/6J Mice1. Biol. Reprod. 24, 784–794. https://doi.org/10.1095/biolreprod24.4.784

Nizari, S., Carare, R.O., Romero, I.A., Hawkes, C.A., 2019. 3D reconstruction of the neurovascular unit reveals differential loss of cholinergic innervation in the cortex and hippocampus of the adult mouse brain. Front. Aging Neurosci. 10. https://doi.org/10.3389/fnagi.2019.00172

Obermeier, B., Daneman, R., Ransohoff, R.M., 2013. Development, maintenance and disruption of the blood-brain barrier. Nat. Med. 19, 1584–1596. https://doi.org/10.1038/nm.3407

Øynebråten, I., Barois, N., Bergeland, T., Küchler, A.M., Bakke, O., Haraldsen, G., 2015. Oligomerized, filamentous surface presentation of RANTES/CCL5 on vascular endothelial cells. Sci. Rep. 5. https://doi.org/10.1038/srep09261

Paganini-hill, A., Henderson, V.W., 1994. Estrogen deficiency and risk of alzheimer's disease in women. Am. J. Epidemiol. 140, 256–261. https://doi.org/10.1093/oxfordjournals.aje.a117244

Pardridge, W.M., Boado, R.J., Farrell, C.R., 1990. Brain-type Glucose Transporter the Blood-Brain Barrier (GLUT- 1) Is Selectively Localized to the Blood-Brain Barrier. J. Biol. Chem. 265, 18035–18040.

Pascual, J.L., Murcy, M.A., Li, S., Gong, W., Eisenstadt, R., Kumasaka, K., Sims, C., Smith, D.H., Browne, K., Allen, S., Baren, J., 2013. Neuroprotective effects of progesterone in traumatic brain injury: Blunted in vivo neutrophil activation at the blood-brain barrier. Am. J. Surg. 206, 840–846. https://doi.org/10.1016/j.amjsurg.2013.07.016

Peinado, M.A., Quesada, A., Pedrosa, J.A., Torres, M.I., Martinez, M., Esteban, F.J., Del Moral, M.L., Hernandez, R., Rodrigo, J., Peinado, J.M., 1998. Quantitative and ultrastructural changes in gila and pericytes in the parietal cortex of the aging rat. Microsc. Res. Tech. 43, 34–42.

https://doi.org/10.1002/(SICI)1097-0029(19981001)43:1<34::AID-JEMT6>3.0.CO;2-G

Peters, A., Josephson, K., Vincent, S.L., 1991. Effects of aging on the neuroglial cells and pericytes within area 17 of the rhesus monkey cerebral cortex. Anat. Rec. 229, 384–398. https://doi.org/10.1002/ar.1092290311

Popescu, B.O., Toescu, E.C., Popescu, L.M., Bajenaru, O., Muresanu, D.F., Schultzberg, M., Bogdanovic, N., 2009. Blood-brain barrier alterations in ageing and dementia. J. Neurol. Sci. 283, 99–106. https://doi.org/10.1016/j.jns.2009.02.321

Ramsauer, M., Krause, D., Dermietzel, R., 2002. Angiogenesis of the blood-brain barrier in vitro and the function of cerebral pericytes. FASEB J. 16, 1274–1276.

Razmara, A., Sunday, L., Stirone, C., Xiao, B.W., Krause, D.N., Duckles, S.P., Procaccio, V., 2008. Mitochondrial effects of estrogen are mediated by estrogen receptor α in brain endothelial cells. J. Pharmacol. Exp. Ther. 325, 782–790. https://doi.org/10.1124/jpet.107.134072

Reeves, M.J., Bushnell, C.D., Howard, G., Gargano, J.W., Duncan, P.W., Lynch, G., Khatiwoda, A., Lisabeth, L., 2008. Sex differences in stroke: epidemiology, clinical presentation, medical care, and outcomes. Lancet Neurol. 7, 915–926. https://doi.org/10.1016/S1474-4422(08)70193-5

Regan, J.C., Partridge, L., 2013. Gender and longevity: Why do men die earlier than women? Comparative and experimental evidence. Best Pract. Res. Clin. Endocrinol. Metab. 27, 467–479. https://doi.org/10.1016/j.beem.2013.05.016

Ribatti, D., Nico, B., Crivellato, E., 2011. The role of pericytes in angiogenesis. Int. J. Dev. Biol. 55, 261–268. https://doi.org/10.1387/ijdb.103167dr

Sandoval, K.E., Witt, K.A., 2011. Age and 17β-estradiol effects on blood-brain barrier tight junction and estrogen receptor proteins in ovariectomized rats. Microvasc. Res. 81, 198–205. https://doi.org/10.1016/j.mvr.2010.12.007

Scheckhuber, C.Q., Wanger, R.A., Mignat, C.A., Osiewacz, H.D., 2011. Unopposed mitochondrial fission leads to severe lifespan shortening. Cell Cycle 10, 3105–3110. https://doi.org/10.4161/cc.10.18.17196

Shimizu, F., Sano, Y., Maeda, T., Abe, M.A., Nakayama, H., Takahashi, R.I., Ueda, M., Ohtsuki, S., Terasaki, T., Obinata, M., Kanda, T., 2008. Peripheral nerve pericytes originating from the blood-nerve barrier expresses tight junctional molecules and transporters as barrier-forming cells. J. Cell. Physiol. 217, 388–399. https://doi.org/10.1002/jcp.21508

Simpson, J.E., Wharton, S.B., Cooper, J., Gelsthorpe, C., Baxter, L., Forster, G., Shaw, P.J., Savva, G., Matthews, F.E., Brayne, C., Ince, P.G., 2010. Alterations of the blood-brain barrier in cerebral white matter lesions in the ageing brain. Neurosci. Lett. 486, 246–251. https://doi.org/10.1016/j.neulet.2010.09.063

Soto, I., Graham, L.C., Richter, H.J., Simeone, S.N., Radell, J.E., Grabowska, W., Funkhouser, W.K., Howell, M.C., Howell, G.R., 2015. APOE Stabilization by Exercise Prevents Aging Neurovascular Dysfunction and Complement Induction. PLoS Biol. 13, 1–33. https://doi.org/10.1371/journal.pbio.1002279

Stewart, P., Magliocco, M., Hayakawa, K., Farrell, C., Del Maestro, R., Girvin, J., Kaufmann, J., Vinters, H., Glibert, J., 1987. A quantitative analysis of blood-brain barrier ultrastructure in the aging human.

Stirone, C., Duckles, S.P., Krause, D.N., Procaccio, V., 2005. Estrogen increases mitochondrial efficiency and reduces oxidative stress in cerebral blood vessels. Mol. Pharmacol. 68, 959–965. https://doi.org/10.1124/mol.105.014662

Sun, N., Yun, J., Liu, J., Malide, D., Liu, C., Rovira, I.I., Holmström, K.M., Fergusson, M.M., Yoo, Y.H., Combs, C.A., Finkel, T., 2015. Measuring In Vivo Mitophagy. Mol. Cell 60, 685–696. https://doi.org/10.1016/j.molcel.2015.10.009

Sure, V.N., Sakamuri, S.S.V.P., Sperling, J.A., Evans, W.R., Merdzo, I., Mostany, R., Murfee, W.L., Busija, D.W., Katakam, P.V.G., 2018. A novel high-throughput assay for respiration in isolated brain microvessels reveals impaired mitochondrial function in the aged mice. GeroScience. https://doi.org/10.1007/s11357-018-0037-8

Sweeney, M.D., Ayyadurai, S., Zlokovic, B. V., 2016. Pericytes of the neurovascular unit: Key functions and signaling pathways. Nat. Neurosci. 19, 771–783. https://doi.org/10.1038/nn.4288

Sweeney, M.D., Sagare, A.P., Zlokovic, B. V., 2018. Blood-brain barrier breakdown in Alzheimer disease and other neurodegenerative disorders. Nat. Rev. Neurol. 14, 133–150. https://doi.org/10.1038/nrneurol.2017.188

Topple, A., Fifkova, E., Baumgardner, D., Cullen-Dockstader, K., 1991. Effect of age on blood vessels and neurovascular appositions in the CA1 region of the rat hippocampus. Neurobiol. Aging 12, 211–217. https://doi.org/10.1016/0197-4580(91)90099-6

Tsai, C.E., Daood, M.J., Lane, R.H., Hansen, T.W.R., Gruetzmacher, E.M., Watchko, J.F., 2002. P-glycoprotein

expression in mouse brain increases with maturation. Biol. Neonate 81, 58–64. https://doi.org/10.1159/000047185

Uspenskaia, O., Liebetrau, M., Herms, J., Danek, A., Hamann, G.F., 2004. Aging is associated with increased collagen type IV accumulation in the basal lamina of human cerebral microvessels. BMC Neurosci. 5, 1–6. https://doi.org/10.1186/1471-2202-5-37

Whittall, C., Kehoe, O., King, S., Rot, A., Patterson, A., Middleton, J., 2013. A Chemokine Self-Presentation Mechanism Involving Formation of Endothelial Surface Microstructures. J. Immunol. 190, 1725–1736. https://doi.org/10.4049/jimmunol.1200867

Wilson, A.C., Clemente, L., Liu, T., Bowen, R.L., Meethal, S.V., Atwood, C.S., 2008. Reproductive hormones regulate the selective permeability of the blood-brain barrier. Biochim. Biophys. Acta - Mol. Basis Dis. 1782, 401–407. https://doi.org/10.1016/j.bbadis.2008.02.011

Winkler, E.A., Bell, R.D., Zlokovic, B. V., 2011. Central nervous system pericytes in health and disease. Nat. Neurosci. 14, 1398–1405. https://doi.org/10.1038/nn.2946

Wolburg, H., Lippoldt, A., 2002. Tight junctions of the blood-brain barrier: Development, composition and regulation. Vascul. Pharmacol. 38, 323–337. https://doi.org/10.1016/S1537-1891(02)00200-8

Yamazaki, Y., Shinohara, Mitsuru, Shinohara, Motoko, Yamazaki, A., Murray, M.E., Liesinger, A.M., Heckman, M.G., Lesser, E.R., Parisi, J.E., Petersen, R.C., Dickson, D.W., Kanekiyo, T., Bu, G., 2019. Selective loss of cortical endothelial tight junction proteins during Alzheimer's disease progression. Brain 142, 1077–1092. https://doi.org/10.1093/brain/awz011

Zlokovic, B. V., 2008. The Blood-Brain Barrier in Health and Chronic Neurodegenerative Disorders. Neuron 57, 178–201. https://doi.org/10.1016/j.neuron.2008.01.003

Figure legends

Fig. 1. Comparison between 2D and 3D analysis of cortical capillaries. A) In the 2D analysis, the BM of aged capillaries was almost twice as thick as the BM of young mice. Aged 3D reconstructed capillaries also showed a significant increase in BM thickness compared to young capillaries from the same region. **B)** Mitochondria were identified as rounded inclusions within the BEC cytoplasm on TEM images and 3D reconstructed vessels. In the 2D analysis, the number and area of mitochondria were significantly decreased in aged BECs. In the 3D analysis, mitochondrial number, but not percentage of

volume per total volume, was significantly decreased in aged vessels. **C)** 2D quantification of pericyte – BEC contact showed no significant differences between ages. However, 3D reconstruction showed a significant increase of pericyte coverage in aged capillaries compared to young capillaries. (n=3 animals/age group, Student's t test; ***, $p<0.001$; *, $p<0.005$; ns, not significant). (Red stars (*): basement membrane; a: astrocyte; bec: brain endothelial cell; m: mitochondria; p: pericyte; tj: tight junction).

Fig. 2. Age-related alterations in 3D reconstructed hippocampal capillaries. A) Aged hippocampal capillaries showed a significant increase in BM thickness when compared to young capillaries from the same region. **B)** Mitochondria were identified as rounded inclusions within the hippocampal BEC cytoplasm, and no significant changes were observed in number and volume between young and aged animals. **C)** 3D reconstruction showed no significant differences in regard to pericyte coverage in aged capillaries compared to young capillaries. (n=3 mice/age group, Student's t test; *, $p<0.05$; ns, not significant).

Fig. 3. BEC pseudopod structural analysis in 3D reconstructed cortical and hippocampal capillaries of young and aged female C57BL/6J mice. Pseudopods were identified as protrusions from the endothelial cytoplasm into the vessel lumen in 3D reconstructed capillaries of young and aged female mice, in both cortex and hippocampus. **A)** Pseudopod number was significantly increased in aged cortical capillaries compared to young cortical capillaries, whereas no changes were observed between aged and young mice in hippocampus. In addition, pseudopod number was significantly greater in aged cortical capillaries compared to aged hippocampal capillaries. **B)** Percentage of pseudopod volume per total cell volume was significantly higher in cortical capillaries from aged animals compared to young cortical capillaries. In contrast, no changes in pseudopod volume were observed between aged and young mice in hippocampus. Additionally, pseudopod volume was significantly greater in aged cortical capillaries compared to aged capillaries from the hippocampus. (n=3 mice/age group, two-way ANOVA and Sidak's correction test; **, ##, $p<0.01$; #, $p<0.05$; ns, not significant).

Fig. 4. Tight junction tortuosity analysis in 3D reconstructed cortical and hippocampal capillaries of young and aged female C57BL/6J mice. Tight junctions were identified alongside the vessel where two BECs overlap in 3D reconstructed capillaries. **A)** Tight junction tortuosity was measured alongside the vessel, taking 3 points (lumen, middle and BM sides of the junction) as reference and obtaining an average value. **B)** Tight junction tortuosity was significantly higher in aged cortical capillaries compared to young cortical capillaries, whereas no changes were observed in hippocampal capillaries. Regional comparisons showed a significantly higher tight junction tortuosity in aged cortical capillaries in comparison to aged hippocampal capillaries. (n=3 mice/age group, two-way ANOVA and Sidak's correction test; ###, $p<0.001$; *, $p<0.05$; ns, not significant).

Fig. 5. Analysis of tight junction complexity in 3D reconstructed cortical and hippocampal capillaries of young and aged female C57BL/6J mice. A) Tight junction complexity was measured by dividing the length of the tight junction by the diagonal of a rectangle containing the whole tight junction. **B)** Tight junction complexity was not significantly changed by age

in cortical or hippocampal capillaries. Regional comparisons showed a small but significant increase in complexity in aged hippocampal capillaries versus aged cortical capillaries. (n=3 mice/age group, two-way ANOVA and Sidak's correction test; #, $p<0.05$; ns, not significant).

Fig. 6. Analysis of pericyte mitochondria in 3D reconstructed cortical and hippocampal capillaries of young and aged female C57BL/6J mice. Mitochondria were identified as rounded inclusions within the pericyte cytoplasm in 2D and 3D reconstructed capillaries in both cortex and hippocampus. **A)** The number of mitochondria did not show significant differences between aged and young capillaries in cortex or hippocampus. **B)** Percentage of mitochondrial volume per total cell volume was significantly increased in aged capillaries of cortex and hippocampus compared to their young counterparts. In some cases, mitochondria were observed to form tubular networks in aged pericytes. In contrast, regional comparisons did not show significant changes in pericytic mitochondrial volume or number between cortical and hippocampal capillaries at any age. (n=3 mice/age group, two-way ANOVA and Sidak's correction test; *, $p<0.05$; ns, not significant). (Red stars (*): basement membrane; a: astrocyte; bec: brain endothelial cell; m: mitochondria; p: pericyte).

Fig. 7. Analysis of the contact between astrocytes and BM in 3D reconstructed cortical and hippocampal capillaries of young and aged female C57BL/6J mice. Astrocytic end-feet were identified as large projections ensheathing the vessel and stablishing contact with the BM of 2D and 3D reconstructed capillaries from cortex and hippocampus. The percentage of astrocyte – BM contact was not significantly changed in aged capillaries compared to young capillaries in cortex or hippocampus. Similarly, astrocyte – BM contact did not show regional differences in any age when comparing cortical and hippocampal capillaries. (n=3 mice/age group, two-way ANOVA and Sidak's correction test; ns, not significant). (Red stars (*): basement membrane; a: astrocyte; bec: brain endothelial cell; m: mitochondria; p: pericyte).

Supplementary Figure legends

Supplemental Fig. 1. Progesterone to estradiol (P:E2) ratio in young and aged C57BL/6J female mice. No significant differences were observed in P:E2 ratio between young female mice in dioestrous and aged female mice. (n=3 mice/age group, Student's t test; ns, not significant).

Supplemental Fig. 2. Classification of oestrous cycle stages in young and comparison with aged C57BL/6J female mice. Phase classification is based on the amount and types of cells present in the vaginal smear. **A)** Pro-oestrous, presence of numerous cells, white arrows point at nucleated epithelial cells (rounded and nucleated) and cornified cells (needle-shaped, dark). **B)** Oestrous, cornified cells and nucleated epithelial cells still appear, white arrow points at non-nucleated epithelial cells (similar shape to nucleated epithelial cells but without nucleus), which start appearing in this phase. **C)** Metoestrous, numerous cornified and non-nucleated epithelial cells are still visible, white arrow points at leukocytes that start appearing in

this phase. **D)** Dioestrous, mainly leukocytes with occasionally some non-nucleated cells. **E)** Vaginal smears of young female mice in dioestrous showed a similar aspect to those of aged acyclic female mice. Scale bars, 50 µm.

Other Supplementary material

Supplemental video 1. A fully reconstructed brain capillary fragment by TEM 3D analysis from a young C57BL/6J female mouse. Orange: astrocyte; yellow: pericyte; purple: brain endothelial cell; green: mitochondria. Square side: 1 µm.

Figure 1

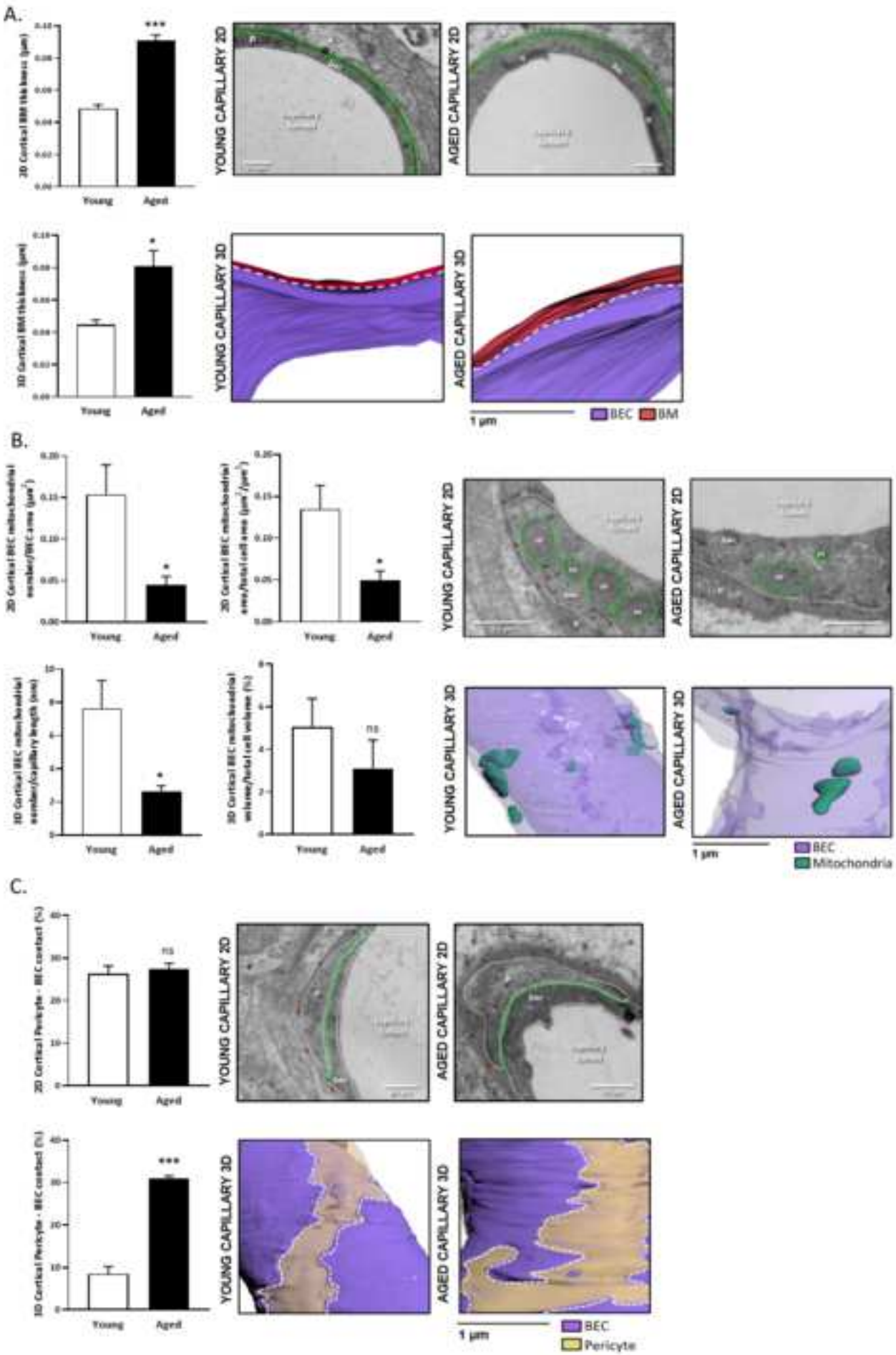

Figure 2

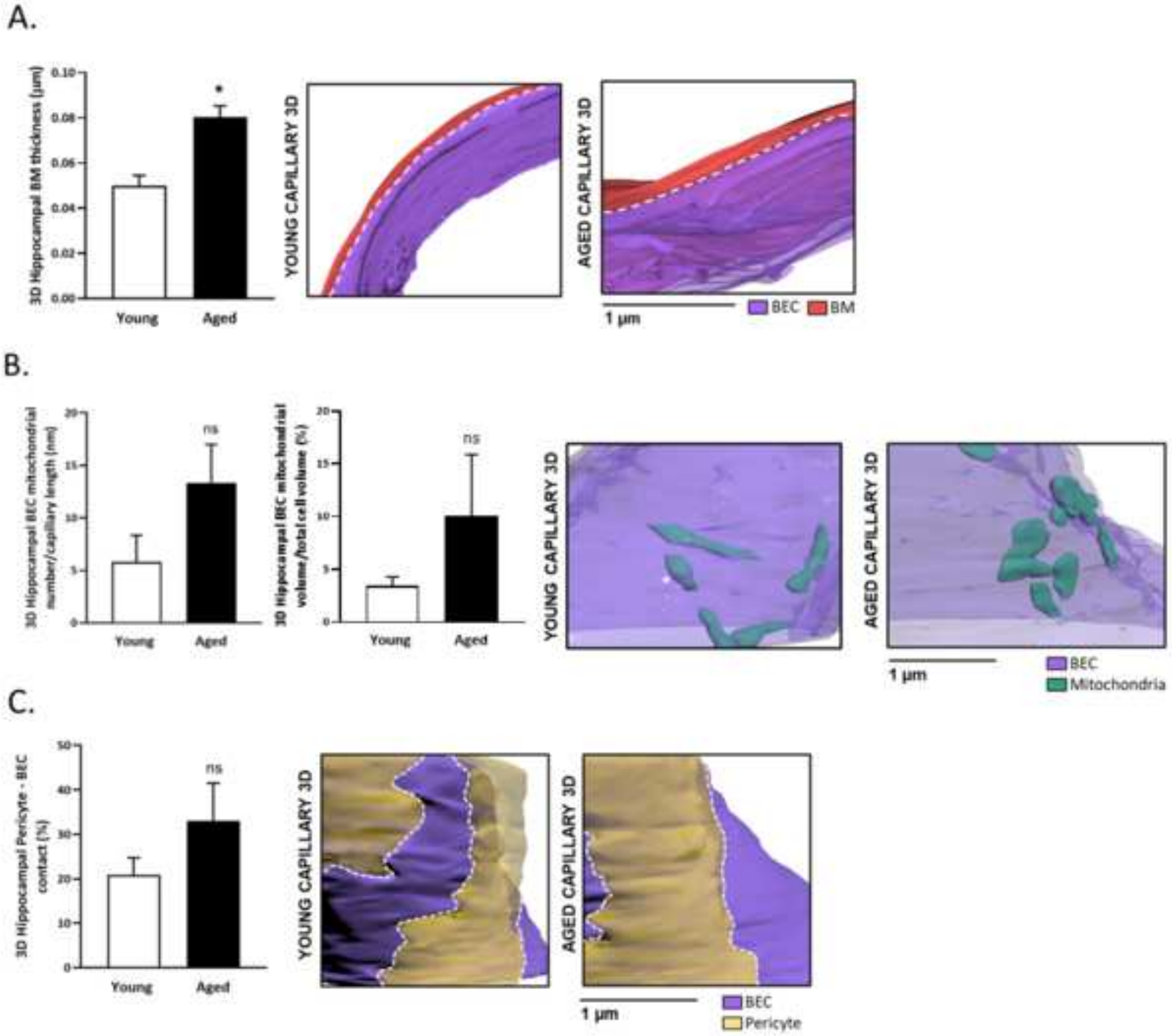

Figure 3

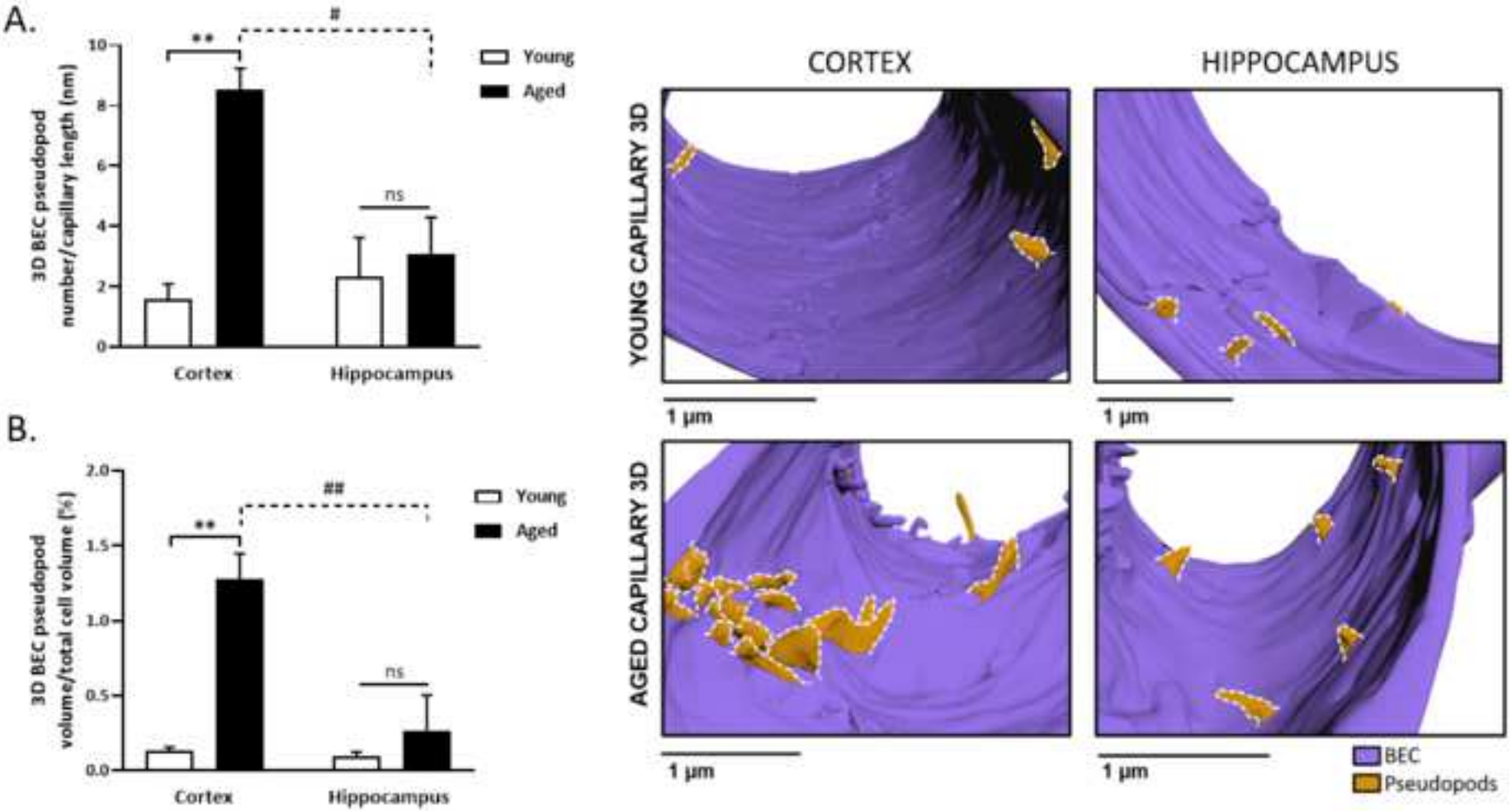

Figure 4

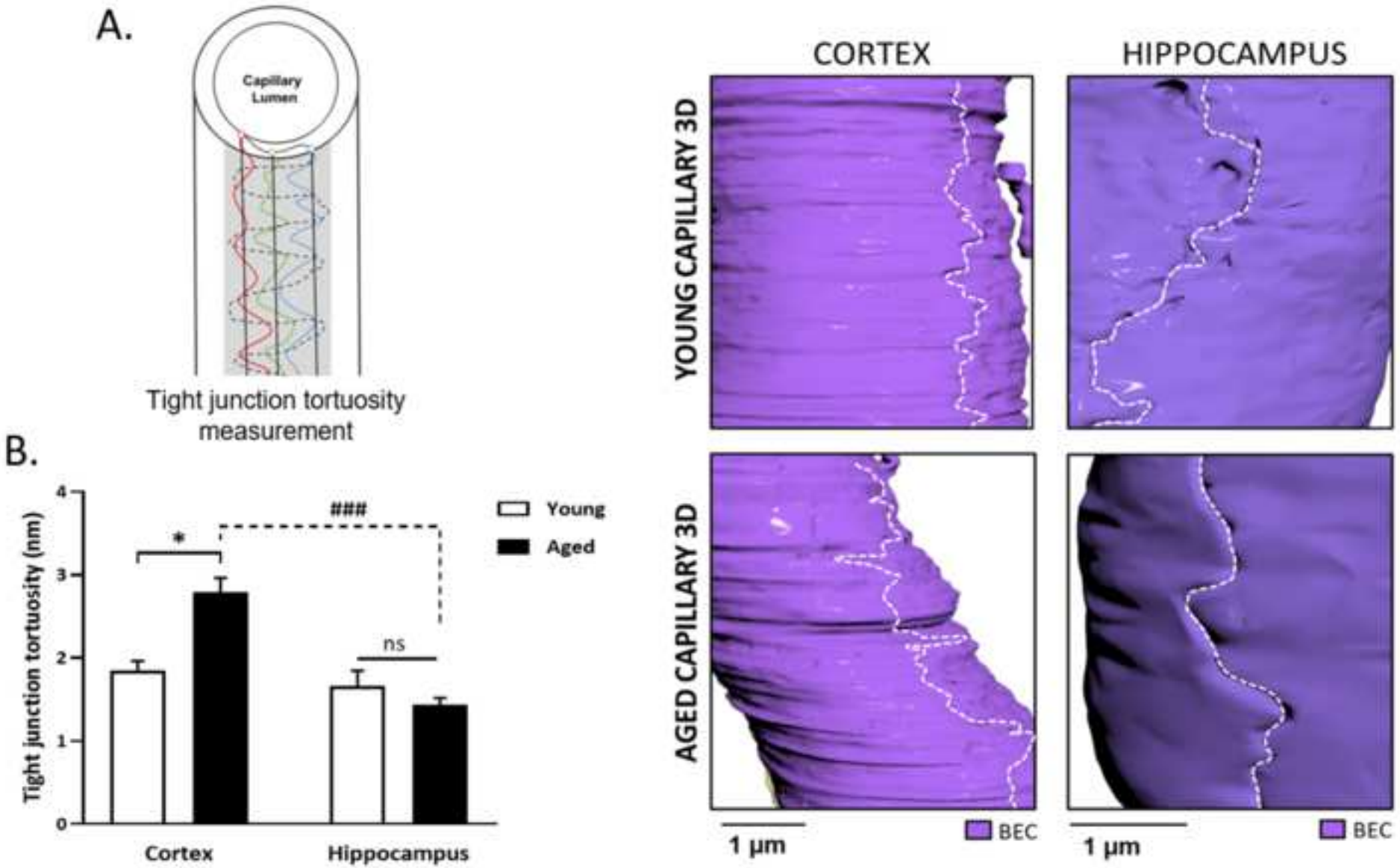

Figure 5

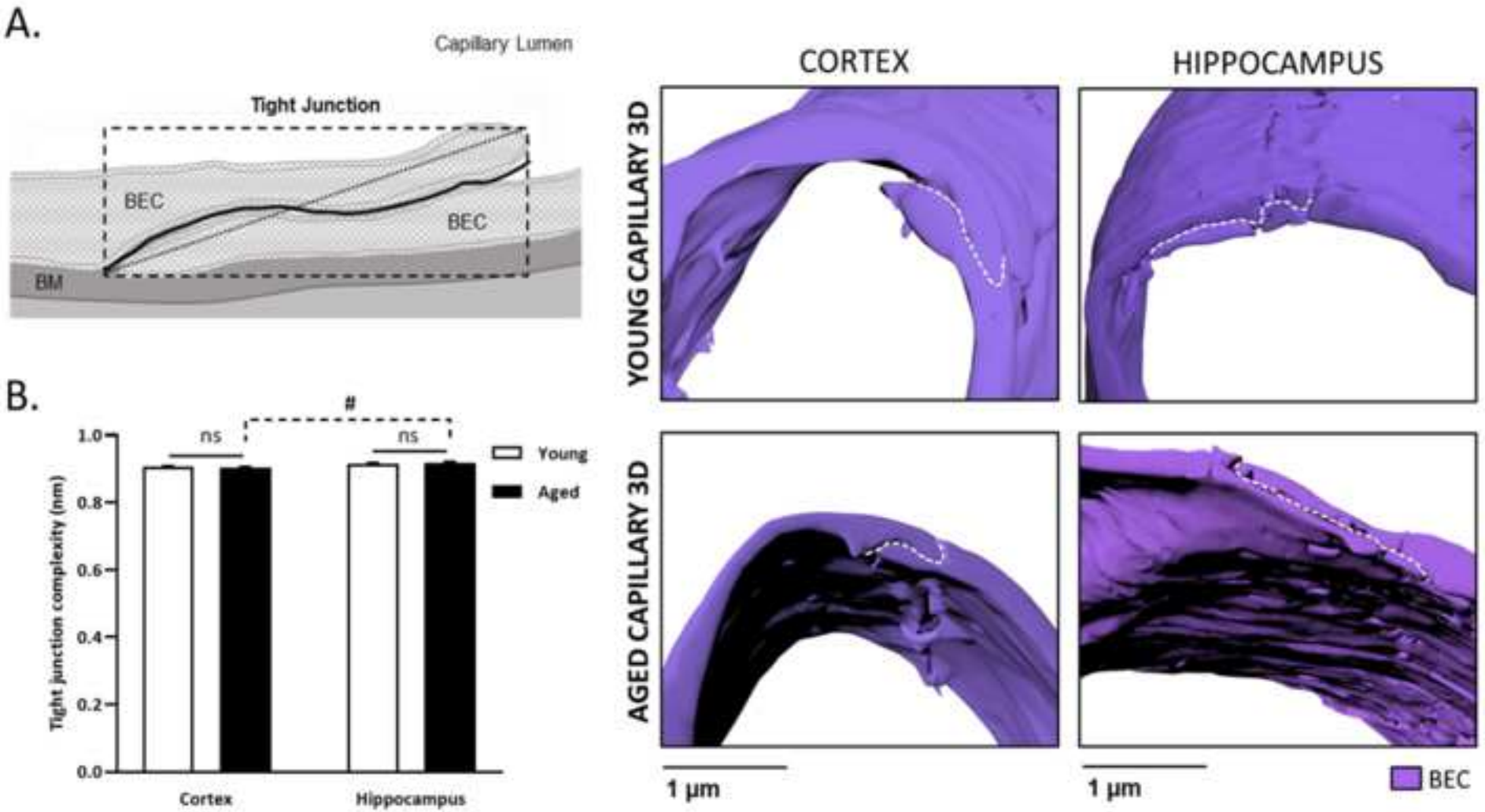

Figure 6

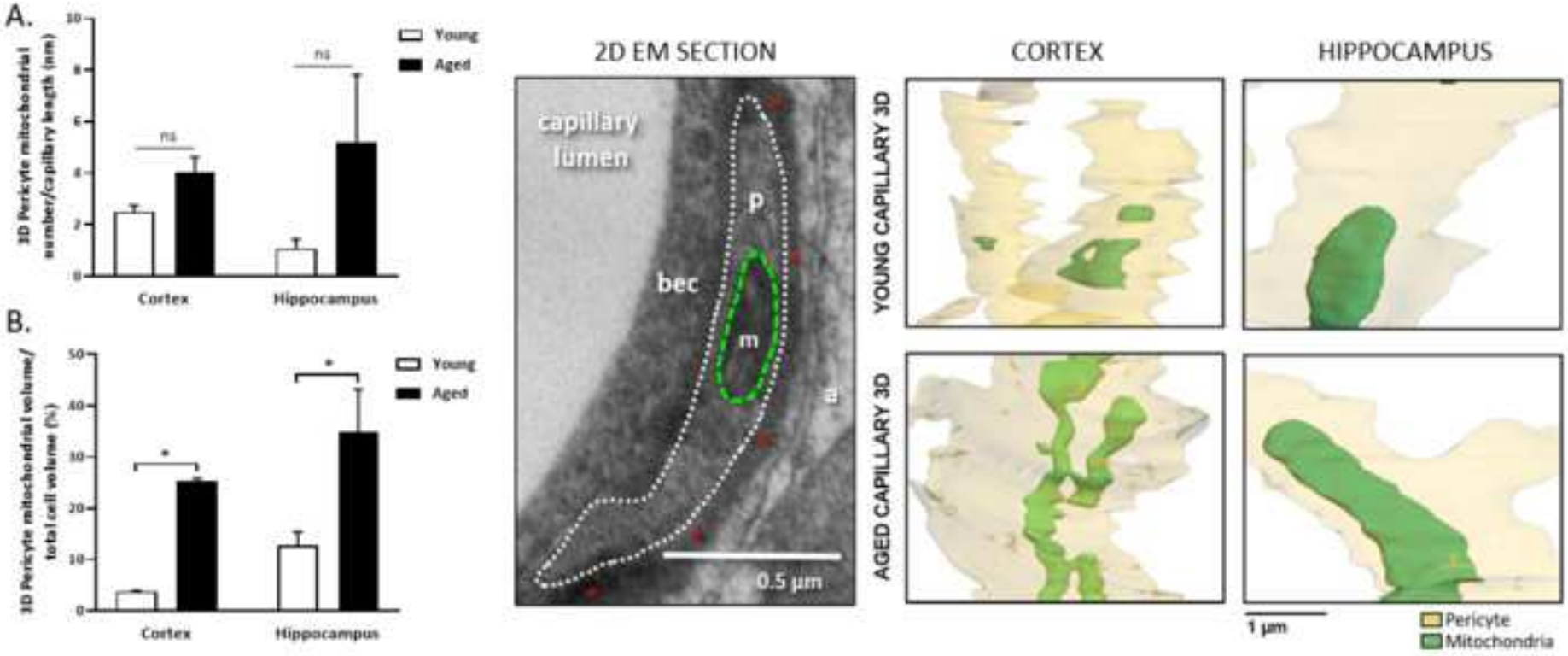

Figure 7

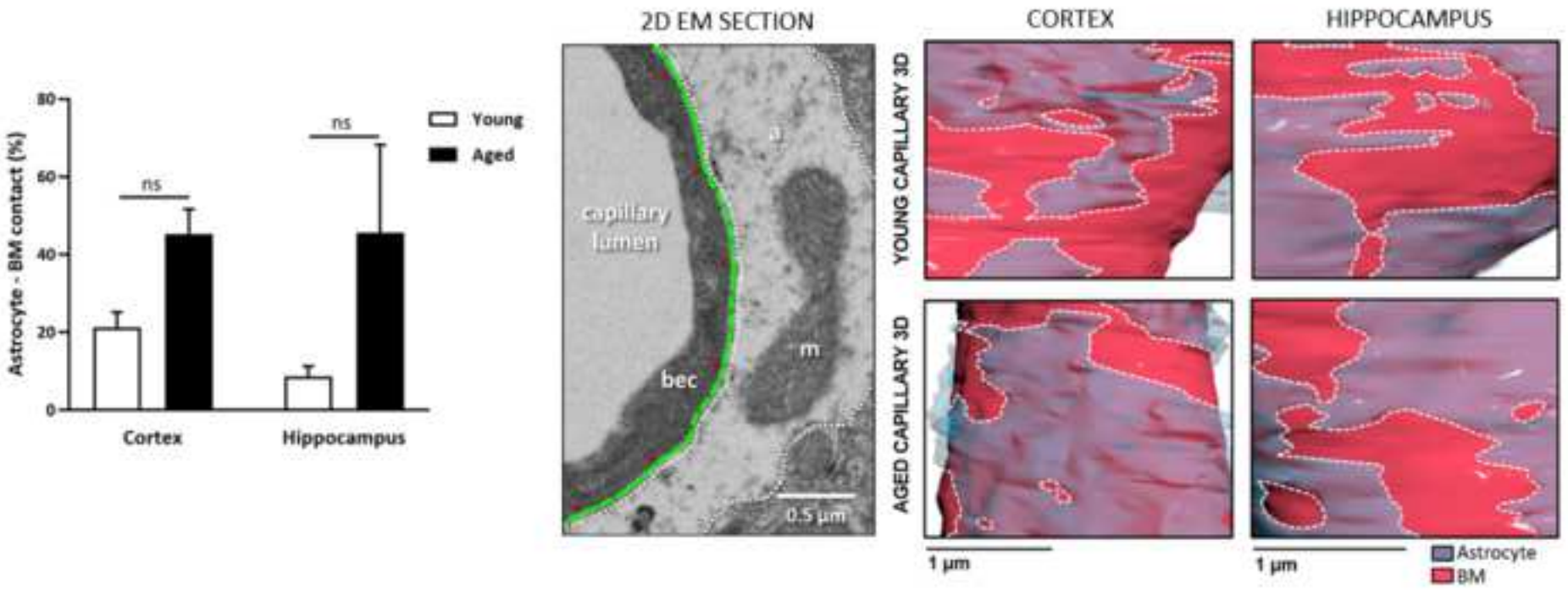

Supplemental Figure 1

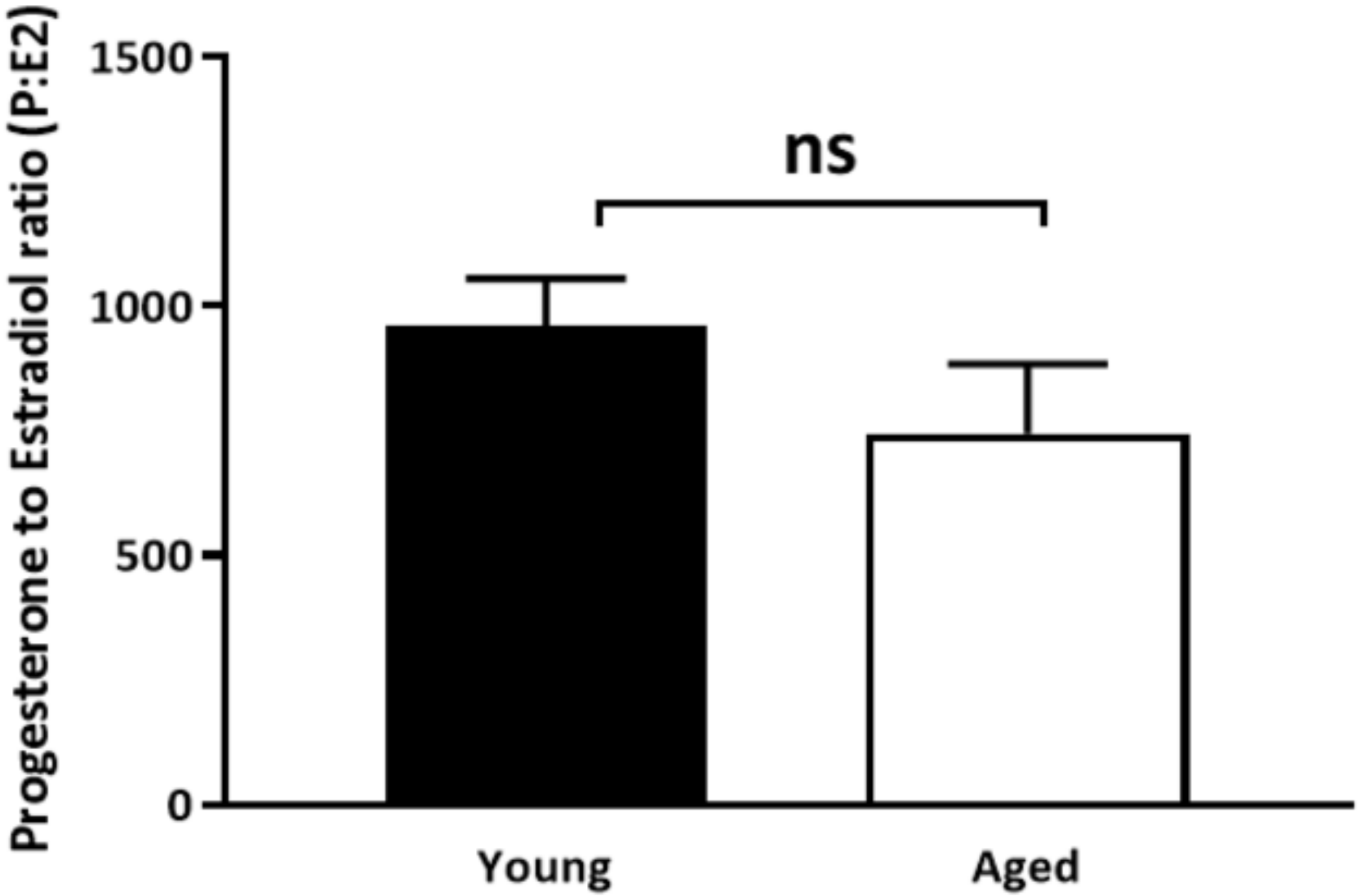

Supplemental Figure 2

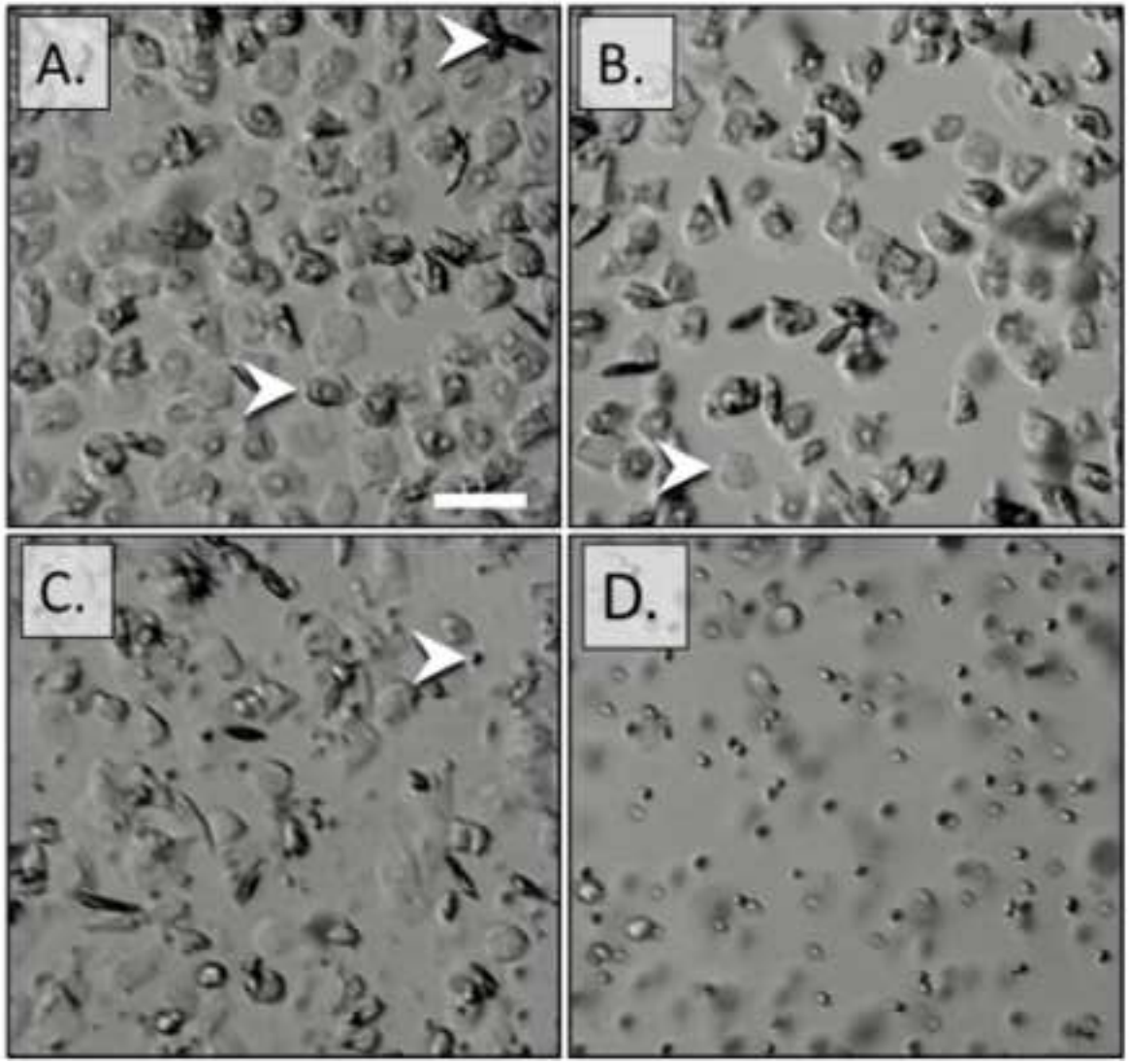

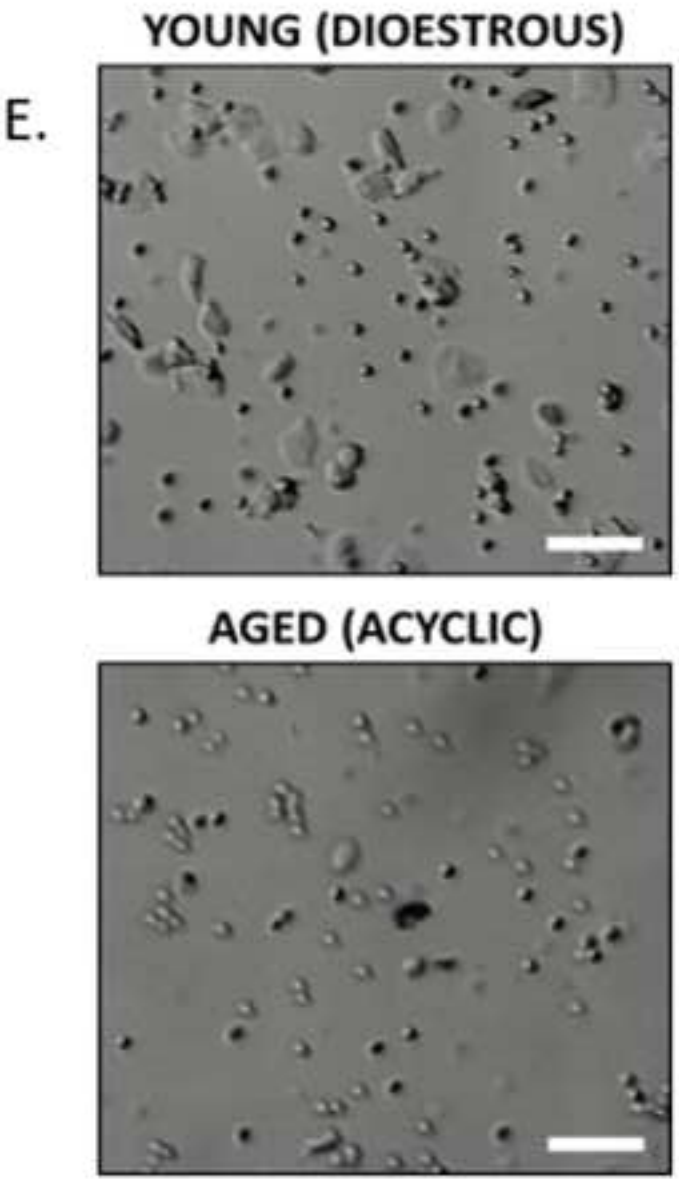

Table 1

Table 1. Comparison between 3D reconstructed cortical and hippocampal capillaries of young and aged female C57BL/6J mice. BM thickness, BEC mitochondrial content and pericyte – BEC contact were measured in 3D reconstructed vessels from cortex and hippocampus. Data is presented as mean ± SEM. *P-values* represent multiple comparisons between young and aged animals (n=3 mice/age group, two-way ANOVA and Sidak's correction test).

	Cortical capillaries			**Hippocampal capillaries**		
Structural features	**Young**	**Aged**	***P*-value**	**Young**	**Aged**	***P*-value**
BM thickness (µm)	0.05 ± 0.003	0.08 ± 0.01	*0.02*	0.05 ± 0.005	0.08 ± 0.005	*0.04*
BEC mitochondrial number per length (number/nm)	7.65 ± 1.66	2.61 ± 0.37	*0.68*	5.82 ± 2.51	13.34 ± 3.65	*0.29*
BEC mitochondrial volume per total volume (%)	5.04 ± 1.34	3.11 ± 1.33	*0.9*	3.43 ± 0.85	10.10 ± 5.78	*0.66*
Pericyte – BEC contact (%)	8.49 ± 1.74	31 ± 0.64	*0.03*	20.85 ± 3.87	33 ± 8.56	*0.14*

Video Still

Click here to access/download;Video Still;Still Image_Video_vessel.tif

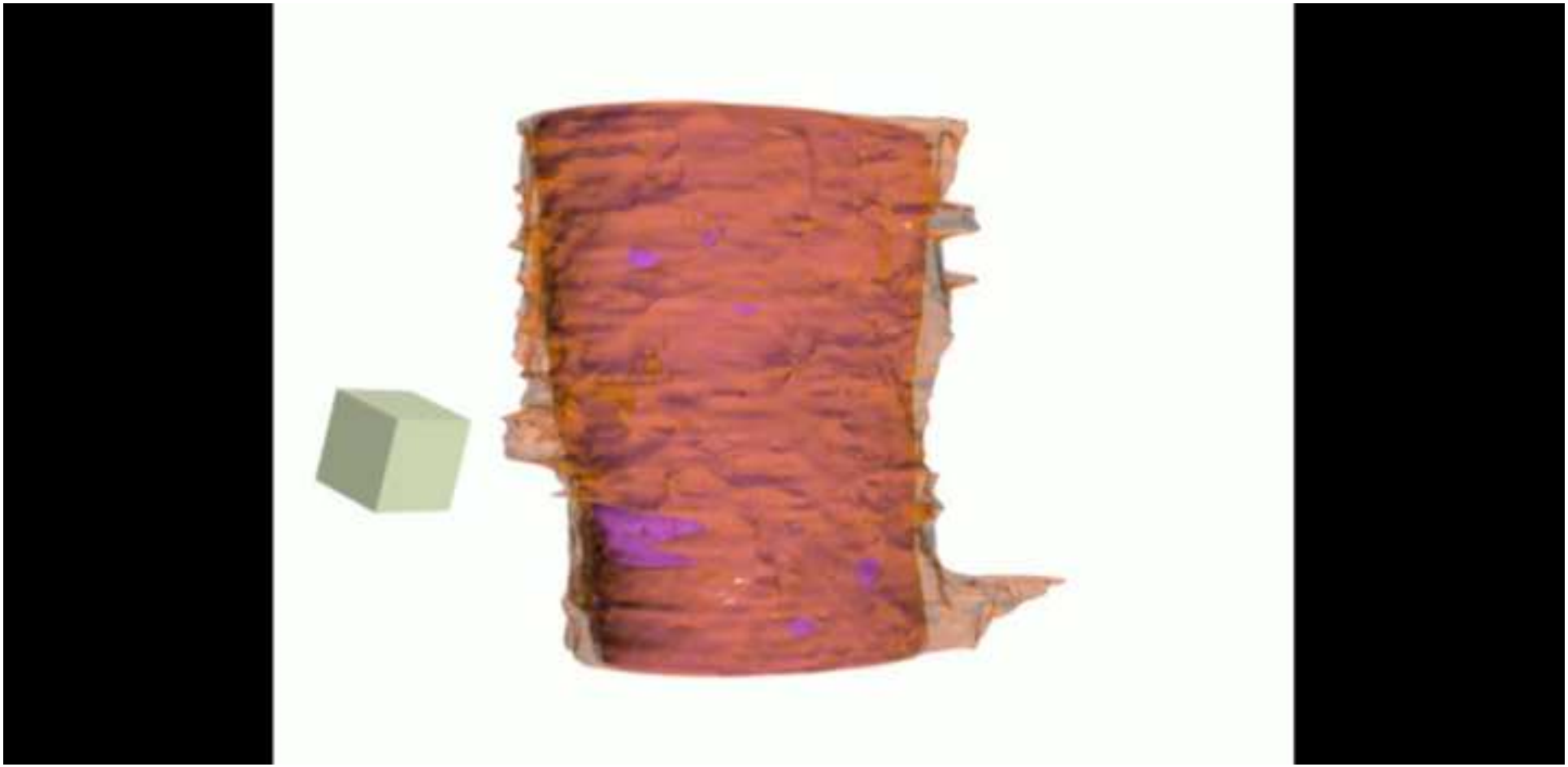

Multimedia File - Video_vessel.avi

This file could not be included in the PDF because the file type is not supported.